Notch pathway activation targets AML-initiating cell homeostasis and differentiation

Camille Lobry,[1,2] Panagiotis Ntziachristos,[1,2] Delphine Ndiaye-Lobry,[1,2] Philmo Oh,[1,2] Luisa Cimmino,[1,2] Nan Zhu,[4,5] Elisa Araldi,[1,2] Wenhuo Hu,[5,7,8] Jacquelyn Freund,[1,2] Omar Abdel-Wahab,[5,6] Sherif Ibrahim,[3] Dimitris Skokos,[9] Scott A. Armstrong,[4,5] Ross L. Levine,[5,6] Christopher Y. Park,[5,7,8] and Iannis Aifantis[1,2,3]

[1]Howard Hughes Medical Institute, [2]Department of Pathology, and [3]NYU Cancer Institute, New York University School of Medicine, New York, NY 10016
[4]Department of Pediatrics; [5]Human Oncology and Pathogenesis Program; [6]Leukemia Service, Department of Medicine; [7]Department of Pathology; and [8]Department of Clinical Laboratories; Memorial Sloan-Kettering Cancer Center, New York, NY 10065
[9]Regeneron Pharmaceuticals, Inc., Tarrytown, NY 10591

Notch signaling pathway activation is known to contribute to the pathogenesis of a spectrum of human malignancies, including T cell leukemia. However, recent studies have implicated the Notch pathway as a tumor suppressor in myeloproliferative neoplasms and several solid tumors. Here we report a novel tumor suppressor role for Notch signaling in acute myeloid leukemia (AML) and demonstrate that Notch pathway activation could represent a therapeutic strategy in this disease. We show that Notch signaling is silenced in human AML samples, as well as in AML-initiating cells in an animal model of the disease. In vivo activation of Notch signaling using genetic Notch gain of function models or in vitro using synthetic Notch ligand induces rapid cell cycle arrest, differentiation, and apoptosis of AML-initiating cells. Moreover, we demonstrate that Notch inactivation cooperates in vivo with loss of the myeloid tumor suppressor Tet2 to induce AML-like disease. These data demonstrate a novel tumor suppressor role for Notch signaling in AML and elucidate the potential therapeutic use of Notch receptor agonists in the treatment of this devastating leukemia.

CORRESPONDENCE
Iannis Aifantis:
iannis.aifantis@nyumc.org
OR
Camille Lobry:
camille.lobry@nyumc.org

Abbreviations used: 4OHT, 4-hydroxytamoxifen; AML, acute myeloid leukemia; ChIP, chromatin immunoprecipitation; CMML, chronic myelomonocytic leukemia; GMP, granulocyte-monocyte progenitor; HSC, hematopoietic stem cell; HSPC, hematopoietic stem and progenitor cell; LIC, leukemia-initiating cell; MLL, mixed lineage leukemia; T-ALL, T cell acute lymphoblastic leukemia; TUNEL, terminal deoxynucleotidyl transferase dUTP nick end labeling.

Notch signaling is a highly evolutionarily conserved pathway implicated in diverse functions including stem cell maintenance, cell fate specification, cell proliferation, and apoptosis. When membrane-bound Notch receptors recognize ligands of the Delta and Jagged families, they are cleaved by metalloproteases and the γ-secretase complex, allowing the release of the intracellular domain into the nucleus where it associates with cofactors to control a significant number of targets including the Hes family of genes (Artavanis-Tsakonas et al., 1999; Ilagan and Kopan, 2007). In the hematopoietic system, Notch is essential for the emergence of definitive hematopoietic stem cells (HSCs) during fetal life (Robert-Moreno et al., 2008) and indispensible for the commitment of progenitors to the T cell lineage (Zúñiga-Pflücker, 2004). Moreover, Notch1 appears to be the central oncogenic trigger in T cell acute lymphoblastic leukemia (T-ALL) in both humans and mice (Weng et al., 2004). Indeed, Notch1 (or its regulator Fbw7) is commonly mutated, leading to constitutive activation of the Notch pathway in the majority of T-ALL patients (Malyukova et al., 2007; Maser et al., 2007; Thompson et al., 2007). In contrast to the T cell lineage where the role of Notch signaling is well defined, there is conflicting information on the role of Notch signaling in the function of adult stem cells (HSCs) and multipotential progenitors and in the myeloerythroid compartment (Maillard et al., 2008; Delaney et al., 2010; Dahlberg et al., 2011). Initial in vitro studies suggested that Notch signaling accelerates

The Rockefeller University Press $30.00
J. Exp. Med. 2013 Vol. 210 No. 2 301-319
www.jem.org/cgi/doi/10.1084/jem.20121484

The Journal of Experimental Medicine

myeloid differentiation (Tan-Pertel et al., 2000; Schroeder et al., 2003). However, subsequent studies contested this conclusion. Most notably, it was shown that Notch can suppress myelopoiesis in vitro (de Pooter et al., 2006), and Mercher et al. (2008) reported that Notch signaling can induce megakaryocyte differentiation. We have recently shown that Notch signaling can function as an antagonist of the granulocyte-monocyte progenitor (GMP) cell fate and that loss of Notch signaling biases commitment toward GMP differentiation, eventually resulting in chronic myelomonocytic leukemia (CMML; Klinakis et al., 2011), a myelodysplastic/myeloproliferative overlap syndrome. We also observed inactivating mutations in the Notch pathway in a fraction of CMML patients, suggesting that this pathway is targeted by genetic alterations. These data are consistent with subsequent reports of inactivating Notch pathway mutations in head and neck cancer (Agrawal et al., 2011; Stransky et al., 2011). However, none of these studies were able to prove that Notch could function as a tumor suppressor in vivo. For example, our data were not able to prove direct involvement of Notch signaling in myeloid disease, as Notch deletion did not lead to transplantable frank myeloid leukemia. They also did not test whether Notch pathway activation can target established disease, something of unique clinical significance.

Acute myeloid leukemia (AML) is a clonal hematopoietic neoplasm characterized by the proliferation and accumulation of myeloid progenitor cells in BM and is the most common acute leukemia diagnosed in adults. Outcomes for AML patients remain poor; despite the use of cytotoxic chemotherapy and stem cell transplantation, most patients die of relapsed, refractory AML (Fröhling et al., 2005). Cytogenetic and molecular studies have shown that AML is a heterogeneous disease in which a variety of cytogenetic and molecular alterations have biological and clinical relevance (Dash and Gilliland, 2001; Armstrong et al., 2003; Döhner et al., 2010). These include chromosomal abnormalities, which lead to the generation of leukemogenic fusion oncoproteins, including mixed lineage leukemia (MLL) gene fusions which are associated with adverse outcome. In addition, somatic mutations in tumor suppressors have been shown to contribute to leukemogenesis and improve AML risk classification (Bacher et al., 2010). However, molecular mechanisms linking these mutations to transformation are incompletely understood, and the role of the most recently identified genes, including *TET2*, *ASXL1*, and *IDH1/2* in AML pathogenesis has not been fully delineated. Current treatments for AML patients include dose-intensive chemotherapy and stem cell transplantation, which are associated with significant toxicities and high relapse rates. Thus, identification of new signaling pathways of which activation or inhibition will lead to therapeutic targeting of AML cells is of urgent clinical significance.

In this study, we analyzed Notch pathway activation status in cytogenetically normal AML patient samples and demonstrated that Notch signaling is silenced in the majority of AML patients. We were also able to demonstrate that reactivation of the Notch signaling pathway both in vivo, using conditional inducible alleles of the active form of *NOTCH1* or *NOTCH2*, as well as in vitro, using recombinant ligand-mediated activation, induced rapid cell cycle arrest, aberrant differentiation, and rapid apoptosis of AML cells. Furthermore, genetic inactivation of Notch signaling combined with deletion of the frequently mutated in AML *TET2* gene (Abdel-Wahab et al., 2009; Delhommeau et al., 2009) collaborated to induce AML-like disease in vivo, strongly suggesting that Notch signaling inhibition is able to promote AML. Our data demonstrate that Notch signaling acts as a tumor suppressor in AML and suggest that Notch reactivation can be used therapeutically in this type of leukemia.

RESULTS

The Notch signaling pathway is silenced in primary AML patient cells

To address the possible involvement of the Notch signaling pathway in AML, we first investigated the status of Notch pathway expression in primary AML patient samples. As we previously showed that Notch/γ-secretase pathway genes are mutated in CMML and that in vivo inactivation of Notch signaling induces CMML-like disease in mice (Klinakis et al., 2011), we focused on acute myelomonocytic leukemias (M4, M4E, and M5 FAB subtypes). We used whole transcriptome data from 187 M4-5 AMLs (Verhaak et al., 2009) and compared them with microarrays from normal Lineage-negative $CD34^+/CD38^-$ human BM hematopoietic stem and progenitor cells (HSPCs; Gentles et al., 2010). As expected, normal HSPCs showed expression of Notch target genes including well-characterized *HES1*, *NRARP*, *DTX1*, and *HEY1* (Fig. 1 A), all direct targets of Notch signaling in hematopoietic cells and other tissues (Palomero et al., 2006; Wang et al., 2011; Ntziachristos et al., 2012). In contrast, Notch activation signature was not observed in most AML samples. Notch receptors also showed a distinct pattern of expression between AML and HSPCs. Whereas *NOTCH1* and *NOTCH2* were highly expressed in HSPCs, NOTCH1 mRNA was expressed significantly less in AML samples (Fig. 1 B). Strikingly, *NOTCH2* mRNA retained high expression in AML samples. Interestingly, we were unable to detect "activated" forms of Notch receptors using Western blotting of primary human AML samples (not depicted), supporting our gene expression experiments and the notion of pathway suppression in this type of leukemia. To address the status of Notch activation in putative leukemia-initiating populations, we purified $CD34^+/CD38^-$ and $CD34^+/CD38^+$ stem/multipotential progenitor populations from AML patients (Table S2) and performed whole genome microarray analysis. We compared expression data from these populations with normal $CD34^+$ BM stem cells and observed that in a fashion similar to our previous experiments (Fig. 1 A), Notch target gene expression was also significantly down-regulated (Fig. 1 C). These data suggest that Notch signaling is also silenced in human AML-initiating cells.

To gain further insights into the mechanisms responsible for Notch pathway silencing in AML samples, we performed

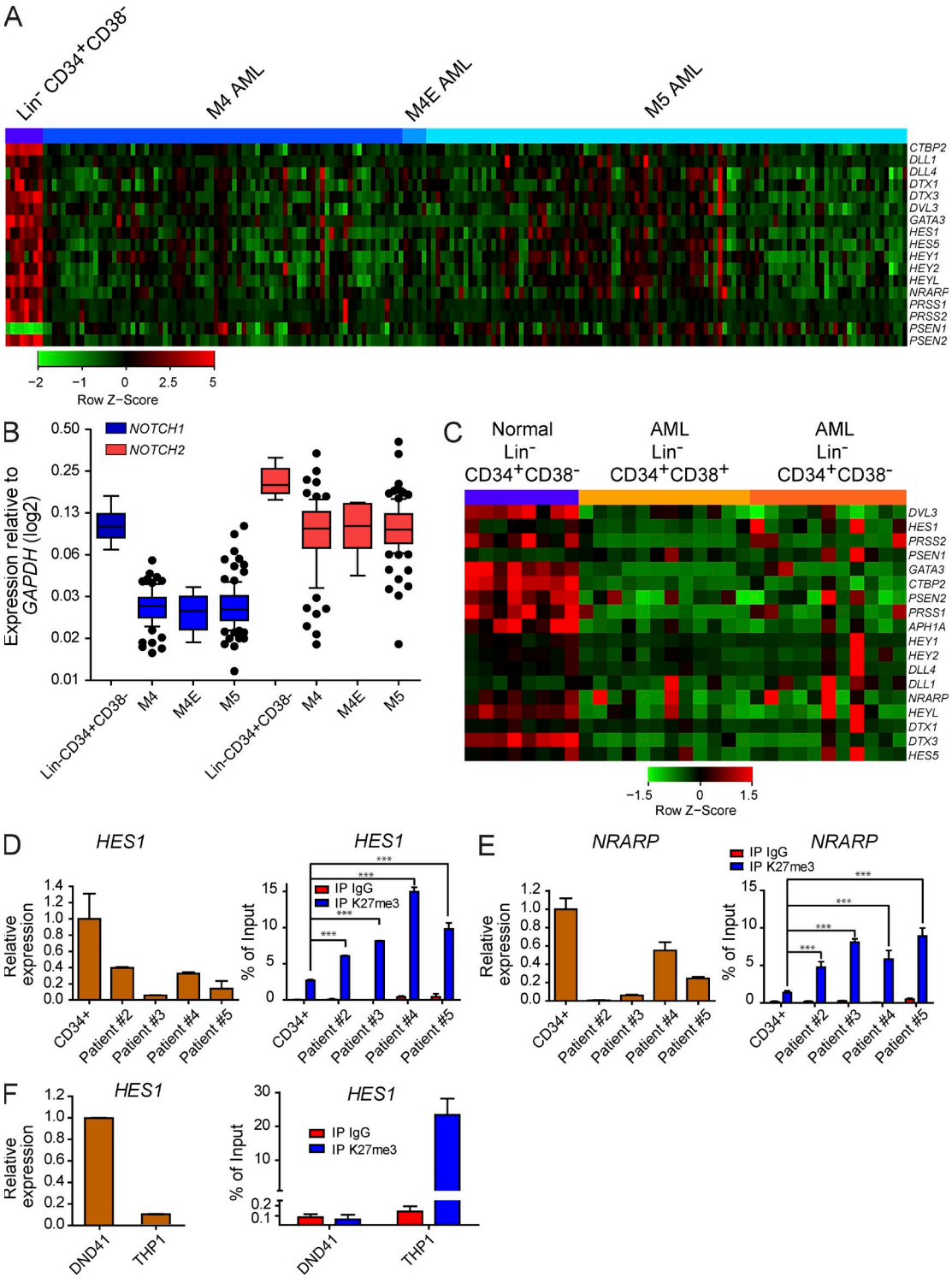

Figure 1. The Notch signaling pathway is silenced in AML patients. (A) Heat map showing relative expression levels of Notch signaling pathway target genes in 187 AML and normal Lin$^-$CD34$^+$CD38$^-$ BM cells. (B) Box plot representing expression value of Notch receptors NOTCH1 and NOTCH2 in the same samples. Expression is normalized to GAPDH expression. (C) Heat map showing relative expression levels of Notch signaling pathway target genes in Lin$^-$CD34$^+$CD38$^-$ and Lin$^-$CD34$^+$CD38$^+$ populations from 12 AML patients compared with normal Lin$^-$CD34$^+$CD38$^-$ BM cells. (D) qRT-PCR analysis for *HES1* gene in CD34$^+$ cord blood stem cells and four AML patient samples (left) and ChIP of H3K27me3 on the promoter of the same samples (right). (E) qRT-PCR analysis for *NRARP* gene in CD34$^+$ cord blood stem cells and four AML patient samples (left) and ChIP of H3K27me3 on the promoter of the same samples (right). (F) qRT-PCR analysis for *HES1* gene in THP1 and DND41 cell lines (left) and ChIP of H3K27me3 on the promoter of *HES1* gene in THP1 and DND41 cell lines (right). (B and D–F) Error bars represent mean ± SD. ***, $P < 0.001$.

Table 1. Characteristics of AML patients used in the study

Patient number	FAB subtype	Cytogenetic	Mutations
1	Non-M3	48,XY,add(4)(p16),+8, der(16)del(16)(p13.1p13.3), del(16)(q22q24)	NC
2	M4E	46,XX,inv(16)(p13.1q22)	NC
3	M1	Normal karyotype 46,XY	FLT3-ITD positive
4	M4E	46,XX,inv(16)(p13.3q22)	NC
5	M4E	46,XY,inv(16)	NPM-1 negative FLT-3 ITD negative
6	M5	Normal karyotype 46,XX	NPM-1 positive FLT-3 ITD positive
7	M1	46,XX, t(4;11) fusion transcripts (e10/e4 and e9/e5)	FLT3 ITD negative

chromatin immunoprecipitation (ChIP) followed by quantitative PCR (qPCR) for the H3K27me3 repressive histone mark at known Notch target loci in AML patient samples of different subtypes (Table 1) and compared them with WT human Lineage$^-$CD34$^+$ cord blood stem/progenitor cells. All tested AML samples showed a marked increase of H3K27me3 abundance on the promoter of the canonical Notch target *HES1* compared with CD34$^+$ cord blood cells (Fig. 1 D, right). This increase in H3K27me3 abundance was tightly correlated with down-regulation of *HES1* gene expression in AML samples revealed by qPCR (Fig. 1 D, left). Increased H3K27me3 was also evident on other canonical Notch target genes including *NRARP* (Fig. 1 E, left) and once again correlated with down-regulation of gene expression (Fig. 1 E, right). We finally investigated H3K27me3 status of *HES1* promoter in the human AML cell line THP1 compared with the Notch-dependent T-ALL cell line DND41. Consistent with our observations in human AML samples, *HES1* promoter showed high increase in H3K27me3 in THP1 cells compared with DND41 cells (Fig. 1 F, right), and this increase was correlated with a reduced expression of the *HES1* gene (Fig. 1 F, left). Accumulation of H3K27me3 at the promoter of Notch target genes is consistent with inactivation of this signaling pathway in AML. Collectively, these data show that Notch signaling is silenced in human AML, excluding a "positive" role for Notch signaling in AML disease progression. Additionally, AML cells specifically express the *NOTCH2* gene, suggesting that Notch signaling could be reactivated in those cells upon ligand binding to the NOTCH2 receptor.

Notch signaling is silenced in an MLL-AF9–driven mouse AML model

To study in vivo the role of Notch signaling in AML, we used the MLL-AF9–driven AML animal model that shares several common features with MLL translocation-driven human AML (Krivtsov et al., 2006). BM HSPCs (Lineage$^-$c-Kit$^+$) were transduced with a retrovirus driving expression of the human MLL-AF9 fusion protein as well as YFP. YFP$^+$ cells were then purified and transplanted into lethally irradiated mice together with a radioprotective dose of WT BM. After disease establishment, mice were sacrificed, and leukemia-initiating cells (LICs) were flow-purified and used for whole transcriptome analysis together with WT Lin$^-$Sca-1$^+$c-Kit$^+$ (LSK) cells and NOTCH1-IC–induced mouse T-ALL primary leukemia cells (Ntziachristos et al., 2012). In mouse MLL-AF9–driven AML, LICs are found in a population phenotypically resembling GMPs but sharing common gene expression with HSCs (Krivtsov et al., 2006) and therefore represent a population of therapeutic importance. Microarray analysis revealed that the Notch gene signature previously used for the study of human AML samples (Fig. 1) was significantly under-represented in mouse AML LICs. The same genes were, as expected, highly expressed in mouse T-ALL cells (Fig. 2 A). The Notch signaling signature was also detected in the LSK population (Fig. 2 A). Consistent with observations made in human AML primary samples, *NOTCH1* expression was low in mouse AML LICs, whereas the *NOTCH2* gene showed an inverse pattern of expression with high expression in LICs (Fig. 2 B). Extracellular staining using NOTCH1- and NOTCH2-specific antibodies followed by FACS analysis confirmed these results at the protein level (Fig. 2 C). To gain further insight into mechanisms responsible for Notch signaling silencing in AML LICs, we assessed ChIP followed by massive parallel sequencing (ChIP-Seq) data for the histone marks H3K4me3 and H3K27me3 (Bernt et al., 2011). Analysis of canonical Notch target genes (*Hes1*, *Nrarp*, and *Gata3*) revealed a significant gain of the H3K27me3 repressive histone mark on each promoter and on gene bodies in the LIC population when compared with the LSK subset (Fig. 2 D). This gain of repressive epigenetic mark was directly correlated to gene expression levels (Fig. 2 E), consistent with a role for H3K27me3 in repression of Notch pathway gene expression. Interestingly, the *NOTCH2* locus did not show a significant increase in H3K27me3 (not depicted). Moreover, H3K4me3 was globally maintained at a high level in LSK and LICs (Fig. 2 D), suggesting that Notch target genes might be poised for activation. Collectively, these data demonstrate that the Notch signaling pathway is silenced in the MLL-AF9–driven mouse model of AML and that AML LICs specifically express *NOTCH2*, suggesting that the Notch signaling pathway can be reactivated.

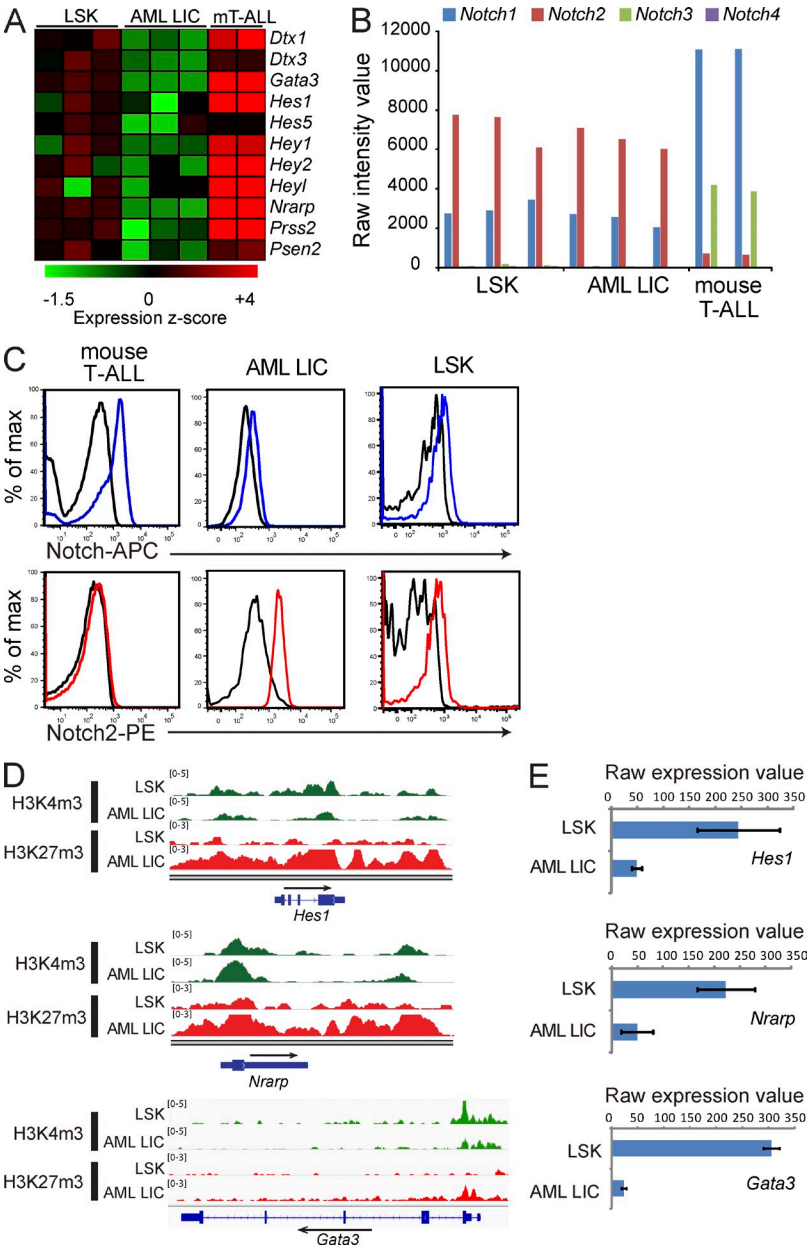

Figure 2. The Notch signaling pathway is silenced in a mouse AML model induced by MLL-AF9. (A) Heat map showing relative expression levels of Notch signaling pathway target genes and Notch receptors in LSK, mouse MLL-AF9–induced AML LICs, and mouse NOTCH1-IC–driven T-ALL cells. (B) Bar graph showing raw expression values of Notch1–4 receptors from different biological replicates of normal mouse LSK population, mouse AML LICs, and T-ALL. (C) FACS analysis using antibodies specific for extracellular domains of Notch1 and Notch2. Black line represents Ig control staining, blue line represents Notch1 antibody, and red line represents Notch2 antibody. (D) ChIP-Seq analysis of H3K4me3 and H3K27me3 on promoter and gene body of Notch target genes *Hes1*, *Nrarp*, and *Gata3* in LSK and AML LICs. (E) Raw expression values of *Hes1*, *Nrarp*, and *Gata3* in LSK and AML LICs. Data represent mean ± SD of three biological replicates.

In vivo activation of Notch signaling suppresses MLL-AF9–induced AML

We next tested whether reactivation of Notch signaling could suppress AML in vivo. We used a conditional knockin model of NOTCH1-IC ($EF1\alpha^{wt/lsl\text{-}N1\text{-}IC}$) crossed to the tamoxifen-inducible ROSA-creERT2 strain. Upon tamoxifen induction, the Notch1-IC transgene is expressed, leading to constitutive activation of the Notch pathway (Buonamici et al., 2009). HSPCs from $EF1\alpha^{wt/lsl\text{-}N1\text{-}IC}$ $ROSA^{wt/CreERT2}$ and $ROSA^{wt/CreERT2}$ littermates were transduced with MLL-AF9-IRES-YFP retrovirus, flow-purified, and transplanted into lethally irradiated congenic recipient together with radioprotective BM. 3 wk after transplantation, mice were bled to assess the state of disease progression and subsequently dosed with tamoxifen. 6 d after tamoxifen administration, a small number of mice was analyzed, and the remaining mice were followed over time for disease progression and survival.

Peripheral blood analysis showed a striking reduction in the proportion of YFP^+ cells and in overall white blood cell counts in NOTCH1-IC–expressing MLL-AF9–positive mice compared with the control cohort (Fig. 3 A). Tissue analysis revealed a significant decrease in spleen size (Fig. 3 C), and further histological analysis showed significantly reduced tissue infiltration in NOTCH1-IC–expressing mice compared with control mice (Fig. 3 B, top). Terminal deoxynucleotidyl transferase dUTP nick end labeling (TUNEL) assay on spleen sections showed a marked increase of apoptotic cells in NOTCH1-IC–expressing cohort (Fig. 3 B, bottom),

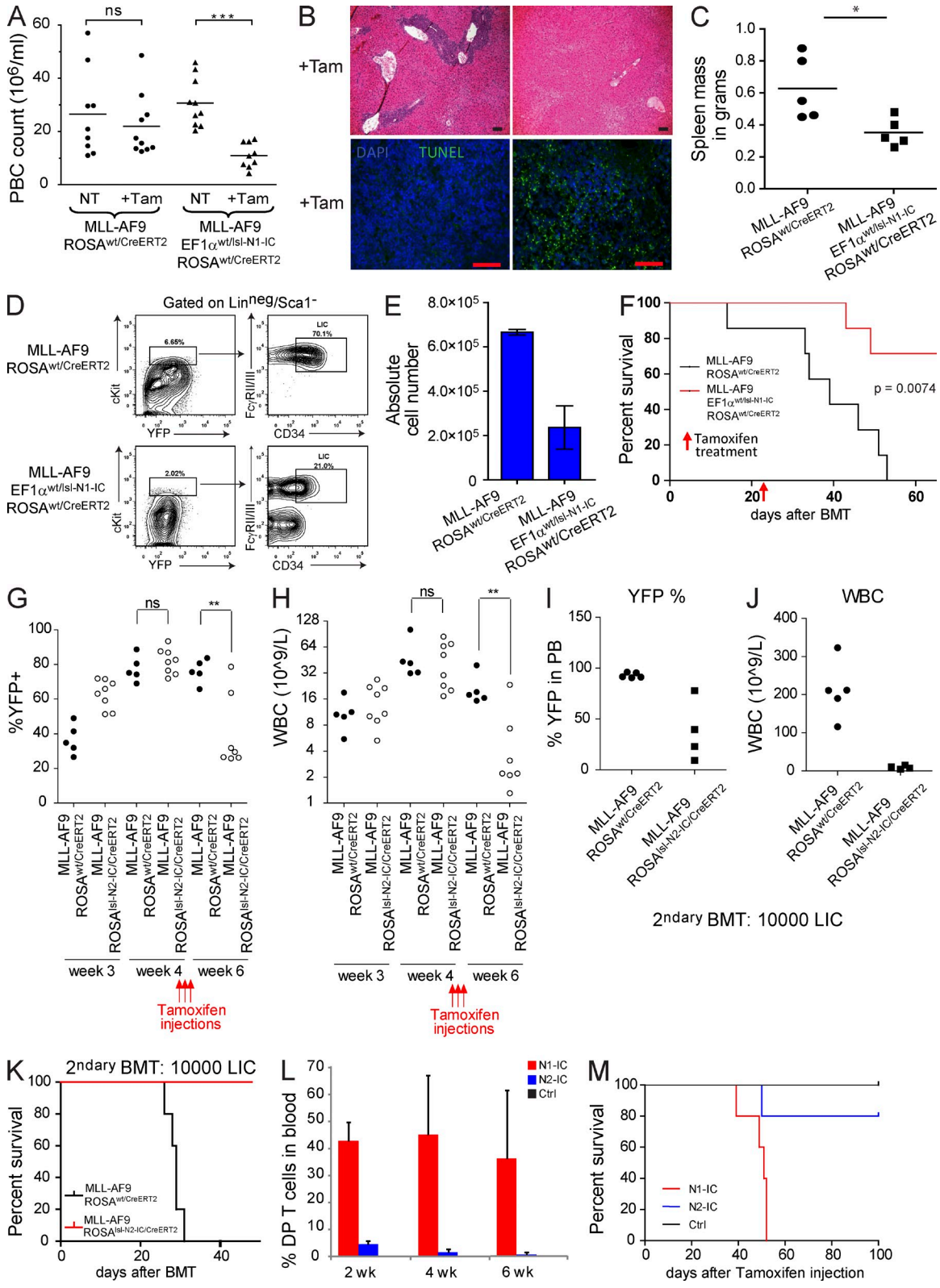

Figure 3. Activation of Notch signaling suppresses AML progression in vivo. (A) Peripheral white blood cell counts before and 6 d after tamoxifen treatment of mice. ***, $P < 0.001$. (B) Representative H&E-stained liver sections from Rosa$^{wt/CreERT2}$ and EF1$\alpha^{wt/lsl\text{-}N1\text{-}IC}$ Rosa$^{wt/CreERT2}$ mice sacrificed 6 d after tamoxifen treatment (top) and representative TUNEL staining on spleen sections from Rosa$^{wt/CreERT2}$ and EF1$\alpha^{wt/lsl\text{-}N1\text{-}IC}$ Rosa$^{wt/CreERT2}$ mice sacrificed 6 d after tamoxifen treatment (bottom). Bars, 200 µm. (C) Mass in grams of spleens from Rosa$^{wt/CreERT2}$ and EF1$\alpha^{wt/lsl\text{-}N1\text{-}IC}$ Rosa$^{wt/CreERT2}$ mice sacrificed 6 d

suggesting that Notch activation induces apoptosis of AML cells in vivo. Most importantly, NOTCH-IC induction resulted in a significant decrease of relative proportion and absolute number of LICs (Fig. 3, D and E) and a significant increase in overall survival compared with control mice (Fig. 3 F; $P < 0.01$). These data demonstrate that in vivo Notch reactivation is able to efficiently suppress AML disease progression by inducing AML cell apoptosis.

As AML cells mainly express NOTCH2 receptor on their surface, similar experiments were performed using an inducible knockin allele of NOTCH2-IC ($Rosa26^{lsl\text{-}N2\text{-}IC/CreERT2}$). HSPCs isolated from $Rosa^{lsl\text{-}N2\text{-}IC/CreERT2}$ and control $Rosa^{wt/CreERT2}$ mice were infected with MLL-AF9 and transplanted in lethally irradiated congenic recipients together with a radioprotective dose of WT BM. After disease establishment, recipient mice were injected three times with tamoxifen. After tamoxifen injection, YFP^+ cells as well as white blood cell count were dramatically reduced in $Rosa^{N2\text{-}IC+/CreERT2}$ MLL-AF9–positive mice compared with control cohort (Fig. 3, G and H). Remaining LICs after tamoxifen injection were sorted and transplanted in sublethally irradiated secondary recipient. 3 wk after transplantation, mice from control cohort ($Rosa^{wt/CreERT2}$ MLL-$AF9^+$) showed highly elevated blood counts with >90% of the peripheral blood cells expressing MLL-AF9 (YFP^+), whereas mice transplanted with $Rosa^{N2\text{-}IC+/CreERT2}$ LICs showed low white blood cell count and low percentage of MLL-AF9–expressing cells (Fig. 3, I and J). Finally, control mice transplanted with LICs purified from $Rosa^{wt/CreERT2}$ died within 30 d after transplantation, whereas mice transplanted with $Rosa^{N2\text{-}IC+/CreERT2}$ survived (Fig. 3 K).

To address potential side effects of Notch2 activation on normal hematopoietic cells, total BM cells from $Rosa^{lsl\text{-}N2\text{-}IC/wt}$ Ubc-CreER, $Rosa^{lsl\text{-}N1\text{-}IC/wt}$, Ubc-creER, and control $Rosa^{wt/wt}$ Ubc-CreER mice were transplanted in lethally irradiated congenic recipients. After engraftment was verified, mice were injected with tamoxifen. As previously reported (Pear et al., 1996), mice with hematopoietic cells expressing N1-IC developed aggressive T-ALL characterized by the abnormal presence of CD4/CD8 double-positive T cells in the peripheral blood (Fig. 3 L). Interestingly, mice with hematopoietic cells expressing N2-IC presented with a low abundant transient wave of CD4/CD8 double-positive T cells in the peripheral blood but didn't develop any sign of acute T cell leukemia. Finally, all the mice expressing N1-IC died of aggressive T-ALL within 60 d after tamoxifen injection, whereas almost all mice expressing N2-IC survived without any signs of T-ALL or other adverse effects (Fig. 3 M). Collectively, these data demonstrate that in vivo activation of the Notch pathway can suppress established AML and suggest that Notch (and specifically Notch2) agonists could be an attractive therapeutic option.

Notch activation targets LIC differentiation and cell survival

To gain additional information into the mechanisms of Notch-mediated AML suppression, LICs from non–tamoxifen-treated $EF1\alpha^{wt/lsl\text{-}NOTCH1\text{-}IC}$ $ROSA^{wt/CreERT2}$ and $ROSA^{wt/CreERT2}$ mice were flow-purified and plated in methylcellulose cultures in the presence of 4-hydroxytamoxifen (4OHT) or DMSO. DMSO-treated LICs showed similar blast colony–forming capacity between $EF1\alpha^{wt/lsl\text{-}NOTCH1\text{-}IC}$ $ROSA^{wt/CreERT2}$ and $ROSA^{wt/CreERT2}$. However, $EF1\alpha^{wt/lsl\text{-}NOTCH1\text{-}IC}$ $ROSA^{wt/CreERT2}$ treated with 4OHT showed a marked decrease of colony number (Fig. 4 B) and loss of blast colony morphology (Fig. 4 A). Cytospin of representative colonies followed by Wright-Giemsa staining revealed that NOTCH1-IC–expressing LICs differentiated to more mature cell fates, with morphology resembling macrophages or DCs (Fig. 4 A). Annexin V staining revealed an increased proportion of cells undergoing apoptosis (Fig. 4 C).

Similar experiments were realized using $ROSA^{lsl\text{-}N2\text{-}IC/CreERT2}$ BM HSPCs infected with MLL-AF9 or AML1-ETO (EA9a). Upon 4OHT treatment and N2-IC expression, MLL-AF9– or AML1-ETO–transformed colonies lost their blast colony morphology and showed a marked significant decrease of colony number (Fig. 4, D and E). Cytospin of representative colonies followed by Wright-Giemsa staining revealed that N2-IC–expressing cells showed morphological changes as they likely differentiated to more mature cell fates (Fig. 4 D).

To further investigate Notch-induced AML LIC differentiation, LICs from $EF1\alpha^{wt/lsl\text{-}N1\text{-}IC}$ $ROSA^{wt/CreERT2}$ and $ROSA^{wt/CreERT2}$ mice were flow-purified 6 d after tamoxifen administration and subjected to gene expression analysis. Gene Set Enrichment Analysis (GSEA) revealed that gene signatures characteristic of macrophage and DC differentiation were significantly enriched in LICs expressing NOTCH1-IC (Fig. 5, A and B). In addition, unsupervised hierarchical clustering using significantly differentially expressed genes showed that

after tamoxifen treatment. *, $P < 0.05$. (A and C) Horizontal lines indicate the mean. (D and E) Representative FACS analysis (gated on $Lin^-/Sca1^-$ cells; D) and absolute number (E) of BM AML LICs. (F) Kaplan-Meier survival analysis of secondary recipients transplanted with 5,000 nontreated LICs from $Rosa^{wt/CreERT2}$ and $EF1\alpha^{wt/lsl\text{-}N1\text{-}IC}$ mice. Tamoxifen was injected once 21 d after transplantation. Each cohort is constituted of seven mice. (G and H) Percentage of YFP^+ peripheral white blood cells (G) and total white blood cell counts (H) before and after tamoxifen treatment of $Rosa^{wt/CreERT2}$ and $Rosa^{lsl\text{-}N2\text{-}IC/CreERT2}$ mice. **, $P < 0.01$. (I and J) Percentage of YFP^+ peripheral white blood cells (I) and total white blood cell counts (J) of secondary recipients transplanted with 10,000 LICs isolated from $Rosa^{wt/CreERT2}$ and $Rosa^{lsl\text{-}N2\text{-}IC/CreERT2}$ mice 3 wk after transplantation. (K) Kaplan-Meier survival analysis of secondary recipients transplanted with 10,000 LICs isolated from $Rosa^{wt/CreERT2}$ and $Rosa^{lsl\text{-}N2\text{-}IC/CreERT2}$ mice. (L) Relative proportion of CD4/CD8 double-positive (DP) T cells in peripheral blood of mice transplanted with total BM from $Rosa^{lsl\text{-}N1\text{-}IC/wt}$ UbcCreER (N1-IC), $Rosa^{lsl\text{-}N2\text{-}IC/wt}$ UbCreERT2 (N2-IC), and UbcCreER (Ctrl) at the indicated time periods after tamoxifen injection of the recipient mice. (E and L) Error bars represent mean ± SD. (M) Kaplan-Meier survival analysis of mice transplanted with total BM from $Rosa^{lsl\text{-}N1\text{-}IC/wt}$ UbcCreER (N1-IC), $Rosa^{lsl\text{-}N2\text{-}IC/wt}$ UbCreERT2 (N2-IC), and UbcCreER (Ctrl; $n = 5$ in each cohort).

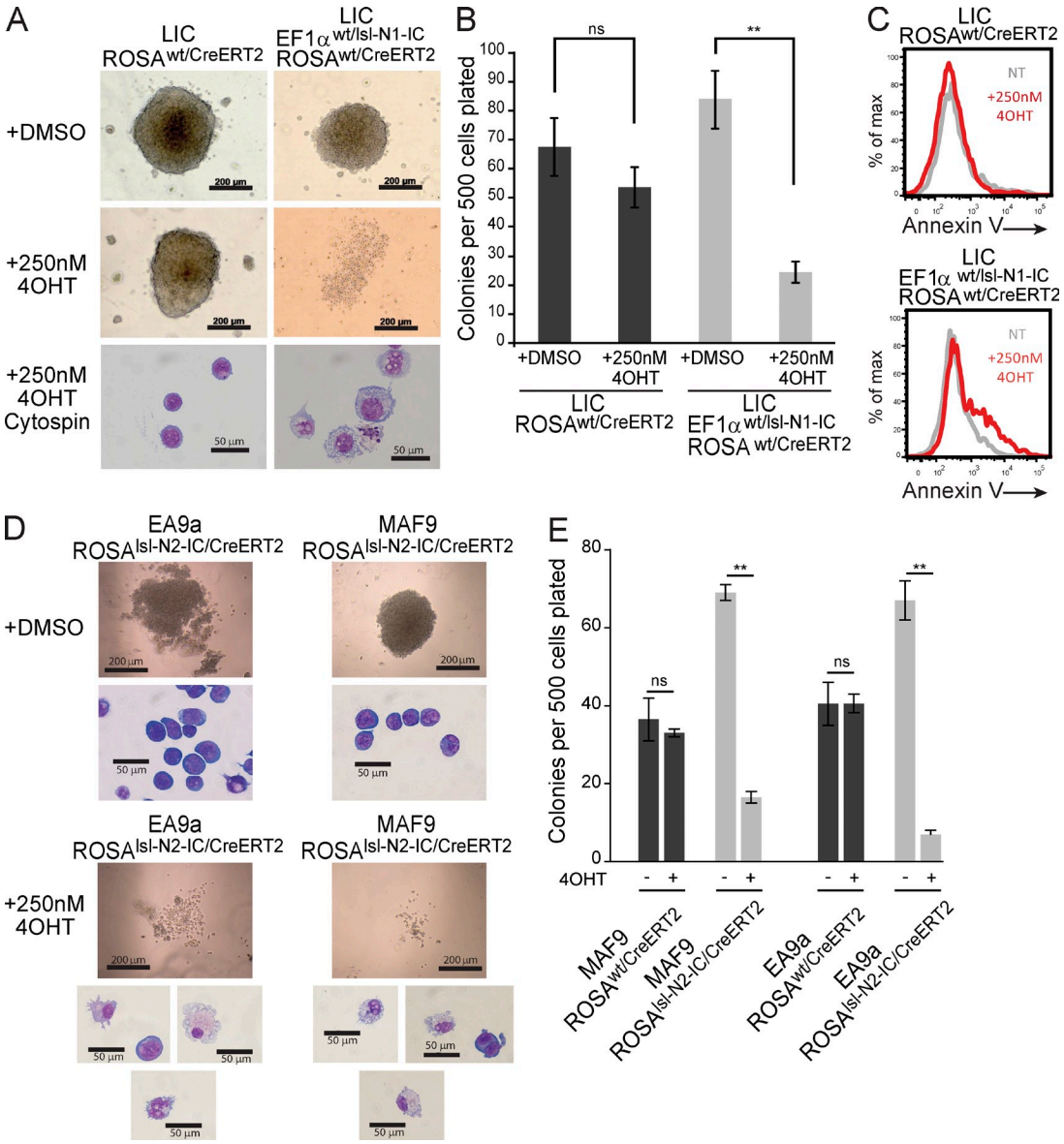

Figure 4. Notch activation induces AML LIC differentiation and apoptosis. (A) Colony morphology in methylcellulose culture and Wright-Giemsa staining of cytospin of LICs from Rosa$^{wt/CreERT2}$ and EF1α$^{wt/lsl-N1-IC}$ mice treated with DMSO or 4OHT. (B) Total colony count of LICs from Rosa$^{wt/CreERT2}$ and EF1α$^{wt/lsl-N1-IC}$ mice treated with DMSO or 4OHT, 8 d after methylcellulose culture initiation. (C) Annexin V staining of LICs from Rosa$^{wt/CreERT2}$ and EF1α$^{wt/lsl-N1-IC}$ mice treated with DMSO or 4OHT, 8 d after methylcellulose culture initiation. (D) Colony morphology in methylcellulose culture and Wright-Giemsa staining of cytospin of MLL-AF9– or AML1-ETO (EA9a)–transformed HSPCs from Rosa$^{lsl-N2-IC/CreERT2}$ mice treated with DMSO or 4OHT. (E) Total colony count of MLL-AF9– or AML1-ETO (EA9a)–transformed HSPCs from Rosa$^{wt/CreERT2}$ and Rosa$^{lsl-N2-IC/CreERT2}$ mice treated with DMSO or 4OHT, 8 d after methylcellulose culture initiation. (B and E) Error bars represent mean ± SD. **, $P < 0.01$. Bars: (A [top and middle] and D [top]) 200 µm; (A and D, bottom) 50 µm.

LICs purified from NOTCH1-IC$^+$ mice cluster closer to spleen macrophages than to control LICs (Fig. 5 C). Further GSEA analysis revealed that LICs expressing NOTCH1-IC down-regulate genes associated with antiapoptotic processes (Fig. 5 A). Microarray results were validated by qRT-PCR, which confirmed up-regulation of genes associated with differentiation (*Adamdec1*, *Cd74*, *Mmp9*, and *Itgax*) and Notch signaling (*Hes1*) and, interestingly, down-regulation of *Bcl2*, a key antiapoptotic effector (Fig. 5 D) recently proposed to play an important role for the propagation of AML (Vo et al., 2012). These experiments demonstrated that Notch signaling activation is able to induce differentiation of the AML leukemia-initiating population toward the macrophage and/or DC lineages, eventually leading to cell death and disease regression in vivo.

Recombinant Notch ligands are able to target mouse and human AML cells

The observation that AML primary samples as well as AML mouse cells express NOTCH2 receptor on the surface

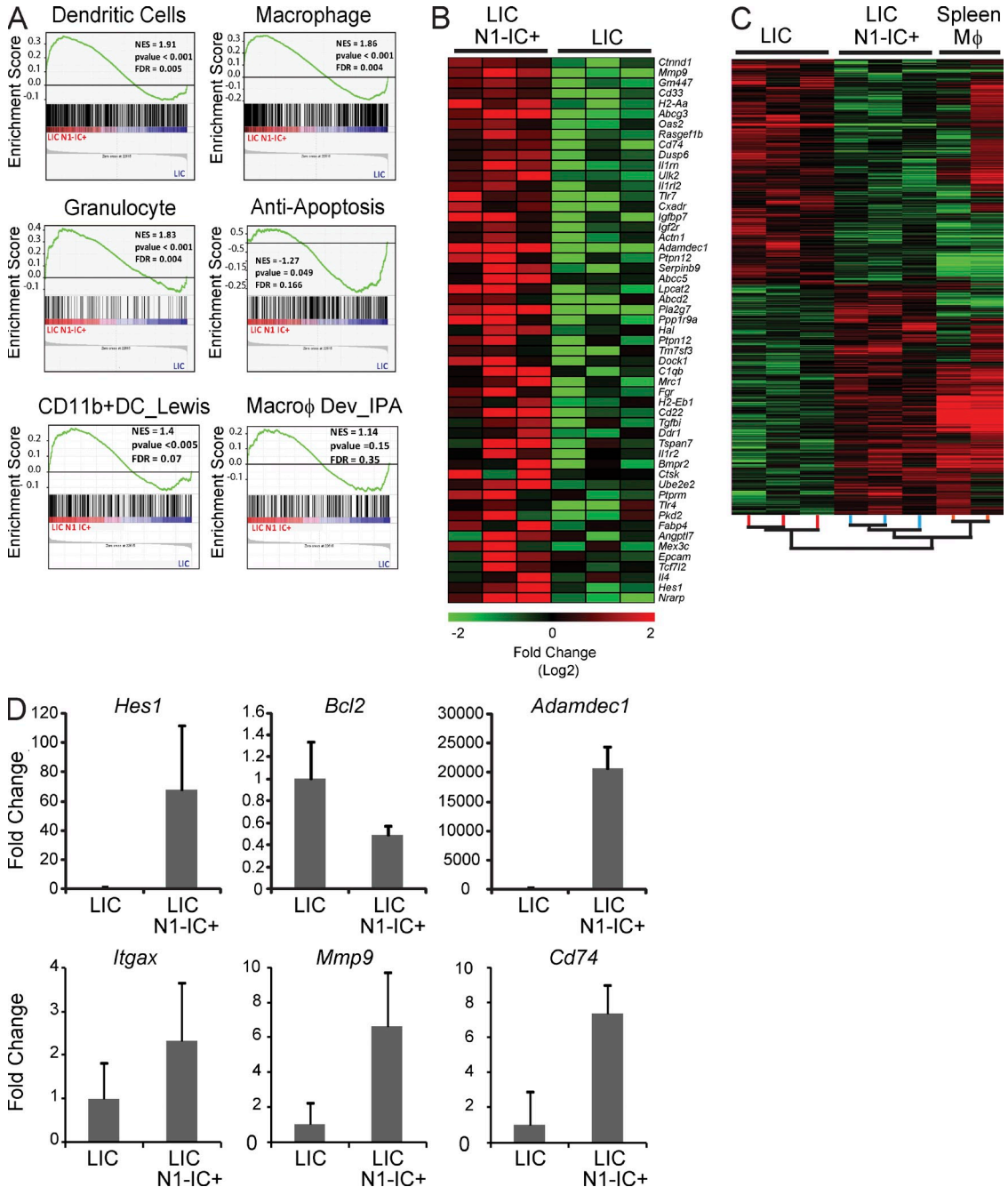

Figure 5. Notch activation induces differentiation-associated genes in AML LICs in vivo. (A) GSEA for the indicated gene sets of LIC N1-IC$^+$ versus LIC. (B) Heat map representing the top significantly up-regulated genes in LIC N1-IC$^+$ compared with LICs. (C) Hierarchical clustering of LICs, LICs expressing NOTCH1-IC (LIC N1-IC$^+$), and spleen macrophages. (D) qRT-PCR of the indicated genes on LICs and LIC N1-IC$^+$. Data represent mean ± SD of three biological replicates.

suggested to us that exogenous activation of Notch signaling could be achieved using Notch receptor ligands/agonists. To test this hypothesis, we cultured mouse AML LICs in the presence of recombinant human Notch ligand Delta-like 4 extracellular domain fused to the IgG-Fc fragment (Dll4-Fc) or with control IgG-Fc. 24 h after culture initiation, Dll4-Fc–treated LICs showed significant changes in cell morphology characteristic of cell differentiation (not depicted). Wright-Giemsa staining showed increased presence of differentiated macrophages and DCs in Dll4-Fc–treated cultures (Fig. 6 A). Cell cycle analysis using Ki67/DAPI staining showed a marked decrease in the proportion of actively cycling cells and a significant increase in cells in G0 and G1 phases of cell cycle (not depicted). Annexin V/7AAD staining revealed a

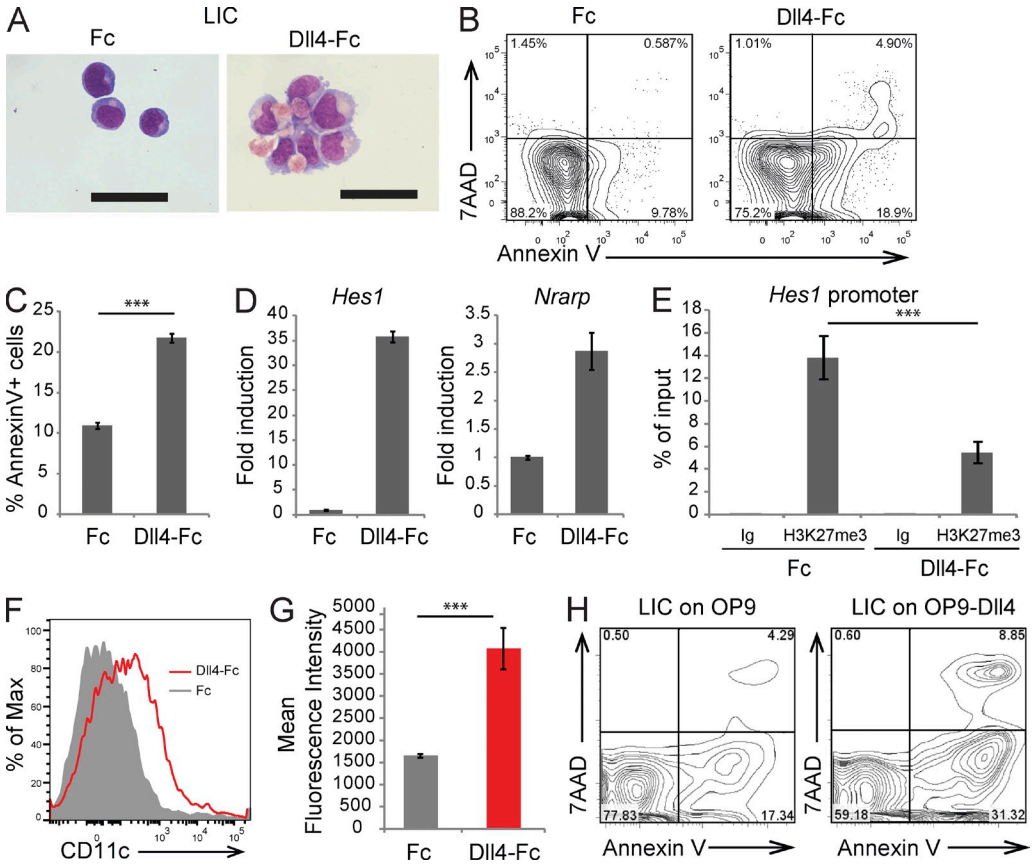

Figure 6. Recombinant Dll4-Fc ligand–mediated Notch activation induces differentiation and apoptosis of AML LICs in vitro. (A) Representative Wright-Giemsa–stained cytospins of LICs treated with Fc control or Dll4-Fc. Bars, 50 µm. (B) Representative FACS staining of apoptosis analysis of LICs treated with Fc control or Dll4-Fc using Annexin V/7AAD FACS staining after 24 h of treatment. (C) Quantification of proportion of apoptotic cells upon Fc or Dll4-Fc treatment. Data represent mean ± SD of three independent experiments. (D) qRT-PCR of the indicated genes in LICs cultured on Dll4-Fc or control Fc for 24 h. (E) ChIP of H3K27me3 on the promoter of *HES1* gene in LICs cultured on Dll4-Fc or control Fc for 24 h. (F) Representative FACS staining for CD11c of LICs treated with Fc control or Dll4-Fc. (G) Mean fluorescence intensity quantification of CD11c staining. (D, E, and G) Data represent mean ± SD of two (E) or three (D and G) biological replicates. (H) Apoptosis analysis of LICs co-cultured with OP9-MIG or OP9-Dll4 using Annexin V/7AAD FACS staining after 48 h of culture. ***, $P < 0.001$.

significant increase of Annexin V–positive cells when stimulated with Dll4-Fc, indicating cell death (Fig. 6, B and C). Notch signaling pathway activation was further confirmed by qPCR showing strong induction of the canonical target genes *Hes1* and *Nrarp* upon Dll4-Fc stimulation (Fig. 6 D). These changes in expression were accompanied by loss of the repressive mark H3K27me3 at the promoter of the *Hes1* gene (Fig. 6 E). Finally, cell surface FACS analysis showed up-regulation of the DC marker CD11c, further confirming induced differentiation in response to Notch ligand treatment (Fig. 6, F and G). These results using recombinant ligand stimulation were further confirmed using co-cultures with OP9 stromal cells expressing Dll4 mouse Notch ligand. Co-culture of freshly purified LICs with OP9-Dll4 lead to significantly increased apoptosis within 48 h after culture initiation when compared with control co-cultures on OP9 cells (Fig. 6 H).

We then asked whether Dll4-Fc–mediated stimulation could also impact human AML cells. We investigated Notch receptor expression in the THP1 and U937 AML cell line by qRT-PCR and extracellular antibody staining and found these cells expressed *NOTCH2* mRNA and protein but no other Notch receptors or downstream targets (Fig. 7, A, C, and G). Human AML cell lines THP1 and U937 were then cultured in the presence of Dll4-Fc or control IgG-Fc for 48 h. Dll4-Fc treatment induced apoptosis of cell lines (Fig. 7, D and I). Morphological observations showed similar trends for cell differentiation as previously observed (Fig. 6) in the treatment of mouse LICs (Fig. 7, B and H). To address whether these effects were specific of Notch activation in myeloid cells and not global toxicity of Notch ligand, we stimulated the Notch-independent T-ALL cell line Loucy with Dll4-Fc or Fc control. Dll4-Fc stimulation was able to induce Hes1 expression (Fig. 7 L) but failed to induce apoptosis in this cell line (Fig. 7 K). These results show that Dll4-Fc–mediated Notch activation induces AML cell line differentiation and apoptosis. Finally, to further prove that these phenotypes are caused by the direct activation of the Notch pathway, we have retrovirally expressed activated forms of Notch2

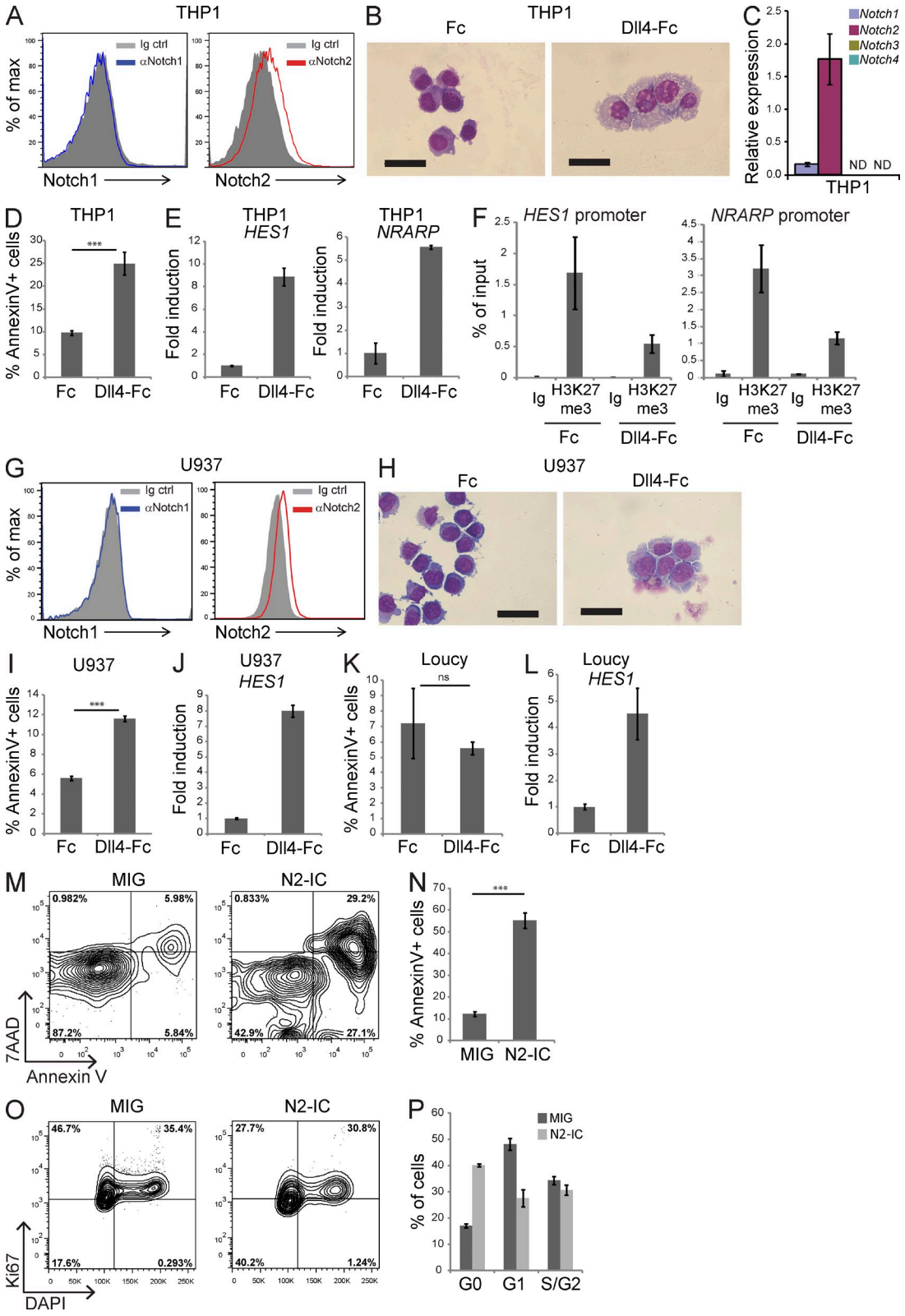

Figure 7. Recombinant Dll4-Fc ligand–mediated Notch activation induces differentiation and apoptosis of THP1 cells. (A) FACS analysis of THP1 using antibodies specific for extracellular domains of Notch1 and Notch2. (B) Representative Wright-Giemsa–stained cytospins of THP1 cells treated with Fc control or Dll4-Fc for 48 h. (C) qRT-PCR analysis of Notch1–4 receptors in THP1 cells. (D) Quantification of proportion of apoptotic THP1 cells by Annexin V staining upon Fc or Dll4-Fc treatment. (E) qRT-PCR of the indicated genes in THP1 cultured on Dll4-Fc or control Fc for 48 h. (F) ChIP of

(NOTCH2-IC) in THP1. In agreement with all other findings, Notch pathway activation led to significant THP1 cell cycle arrest and apoptosis induction (Fig. 7, M–P).

To gain further insights into mechanisms responsible for AML cell differentiation and apoptosis, we performed whole transcriptome profiling of untreated or Dll4-Fc–treated THP1 AML cells. As observed previously for in vivo purified mouse AML LICs expressing NOTCH1-IC (Fig. 5), GSEA analysis showed that THP1 treated with Dll4-Fc up-regulate gene signatures associated with macrophage and DC differentiation (Fig. 8, A and B) and down-regulated gene signatures associated with leukemic stem cell maintenance. Interestingly, THP1 cells treated with Dll4-Fc and mouse LICs purified after in vivo Notch pathway activation shared common gene expression signatures, suggesting a high degree of conservation between mouse and human AML cellular response to Notch agonists (Fig. 8 B, gene set "Top genes AML LIC N1-IC"). Microarray results were further validated using qRT-PCR. In agreement with previous results using mouse LICs expressing NOTCH1-IC (Fig. 5), THP1 AML cells treated with Dll4-Fc up-regulated differentiation-associated genes (*ADAMDEC1*, *CD74*, *MMP9*, and *ITGAX*) and down-regulated *BCL2* (Fig. 8 C). Interestingly, THP1 treated with Dll4-Fc also significantly up-regulated the cell cycle inhibitor p21 (*CDKN1A*).

Notch reactivation induces human primary AML sample differentiation and apoptosis

These promising results using Notch ligand stimulation of mouse and human AML cell lines led us to then test whether primary cells from AML patients could be similarly affected. AML samples from different subtypes (Table 1) were cultured in the presence of Dll4-Fc or control vehicle in serum-free expansion medium supplemented with cytokines for 24 h. Apoptosis state was then monitored using Annexin V FACS staining. Samples treated with Dll4-Fc showed significant increase in levels of Annexin V staining, suggesting increased programmed cell death (Fig. 8 D). Additionally, some samples showed altered morphology as already observed for mouse LICs or THP1 stimulated with Dll4-Fc (Fig. 8 E). NOTCH2 receptor surface expression was confirmed by antibody staining followed by flow cytometry analysis (Fig. 8 F), and activation of Notch signaling pathway was confirmed by qPCR showing strong induction of the canonical target gene *HES1* (Fig. 8 G). These results show that Notch activation using recombinant ligand can induce AML patient cell differentiation and apoptosis.

Combined Notch and Tet2 inactivation leads to AML-like disease in vivo

All of these experiments suggest a novel tumor suppressor function for Notch signaling in AML. We have recently shown that Notch inactivation leads to a CMML-like myeloproliferative disease (myeloproliferative neoplasm) but is not sufficient to induce AML (Klinakis et al., 2011). We therefore hypothesized that loss of Notch signaling might collaborate with other oncogenic lesions to induce AML and noticed that 80% of CMML patients carrying Notch pathway mutations also harbor inactivating mutations in the *TET2* gene, which is frequently mutated in myeloproliferative neoplasm and AML (Abdel-Wahab et al., 2009; Delhommeau et al., 2009; Langemeijer et al., 2009). We have thus focused on the potential functional collaboration of the two genetic events. We and others have recently shown that genetic inactivation of Tet2 in mice also leads to a CMML-like disease, but not overt AML, in the first 6–10 mo after gene deletion (Ko et al., 2011; Li et al., 2011; Moran-Crusio et al., 2011; Quivoron et al., 2011). To address whether Notch and Tet2 loss of function could collaborate to induce AML in vivo, we generated compound knockout animals ($Ncstn^{f/f}Tet2^{f/f}$). Deletion of *Ncstn* and *Tet2* was induced using the hematopoietic-specific Vav1-cre deleter strain (Stadtfeld and Graf, 2005). Peripheral blood analysis of $Ncstn^{-/-}Tet2^{-/-}$ mice at 7 wk after birth showed a significant increase in whole white blood cell counts and absolute number of myelomonocytic cells ($CD11b^{+}/Gr1^{+}$; Fig. 9, A and B), whereas $Tet2^{-/-}$ and $Ncstn^{-/-}$ control animals showed no signs of induced disease at this early time point (Fig. 9 B). Differential counts using Wright-Giemsa–stained peripheral blood smears revealed a high proportion (>20%) of blast-like cells (Fig. 9 C), whereas only differentiated monocytes and granulocytes could be observed in $Ncstn^{-/-}$ or $Tet2^{-/-}$ single knockout animals (Klinakis et al., 2011; Moran-Crusio et al., 2011).

$Ncstn^{-/-}Tet2^{-/-}$ compound animals presented with significantly enlarged spleens (Fig. 9 D), and histological and FACS analysis of tissues showed massive infiltration of both differentiated and blast-like myeloid cells (Fig. 9, E and F; and not depicted). Detailed FACS analysis of the BM myeloid

H3K27me3 on the promoter of *HES1* and *NRARP* genes in THP1 cells cultured on Dll4-Fc or control Fc for 24 h. (G) FACS analysis of U937 cells using antibodies specific for extracellular domains of Notch1 and Notch2. (H) Representative Wright-Giemsa–stained cytospins of U937 cells treated with Fc control or Dll4-Fc for 48 h. Bars, 50 µm. (I) Quantification of proportion of apoptotic U937 cells by Annexin V staining upon Fc or Dll4-Fc treatment. (J) qRT-PCR of *HES1* gene in U937 cells cultured on Dll4-Fc or control Fc for 48 h. (K) Quantification of proportion of apoptotic Loucy cells by Annexin V staining upon Fc or Dll4-Fc treatment. (D, I, and K) Data represent mean ± SD of three independent experiments. (L) qRT-PCR of *HES1* gene in Loucy cells cultured on Dll4-Fc or control Fc for 48 h. (M) Representative apoptosis analysis of THP1 using Annexin V/7AAD FACS staining 6 d after infection with pMIG or pMIG-NOTCH2-IC. (N) Quantification of proportion of apoptotic THP1 cells 6 d after infection with pMIG or pMIG-NOTCH2-IC (N2-IC). Error bars represent mean ± SD. (O and P) Representative cell cycle analysis of THP1 using Ki67 and DAPI FACS staining (O) and quantification of proportion of cells in each cell cycle phase (P) 6 d after infection with pMIG or pMIG-NOTCH2-IC (N2-IC). (C, E, F, J, L, and P) Data represent mean ± SD of two (F) or three (C, E, J, L, and P) biological replicates. ***, $P < 0.001$.

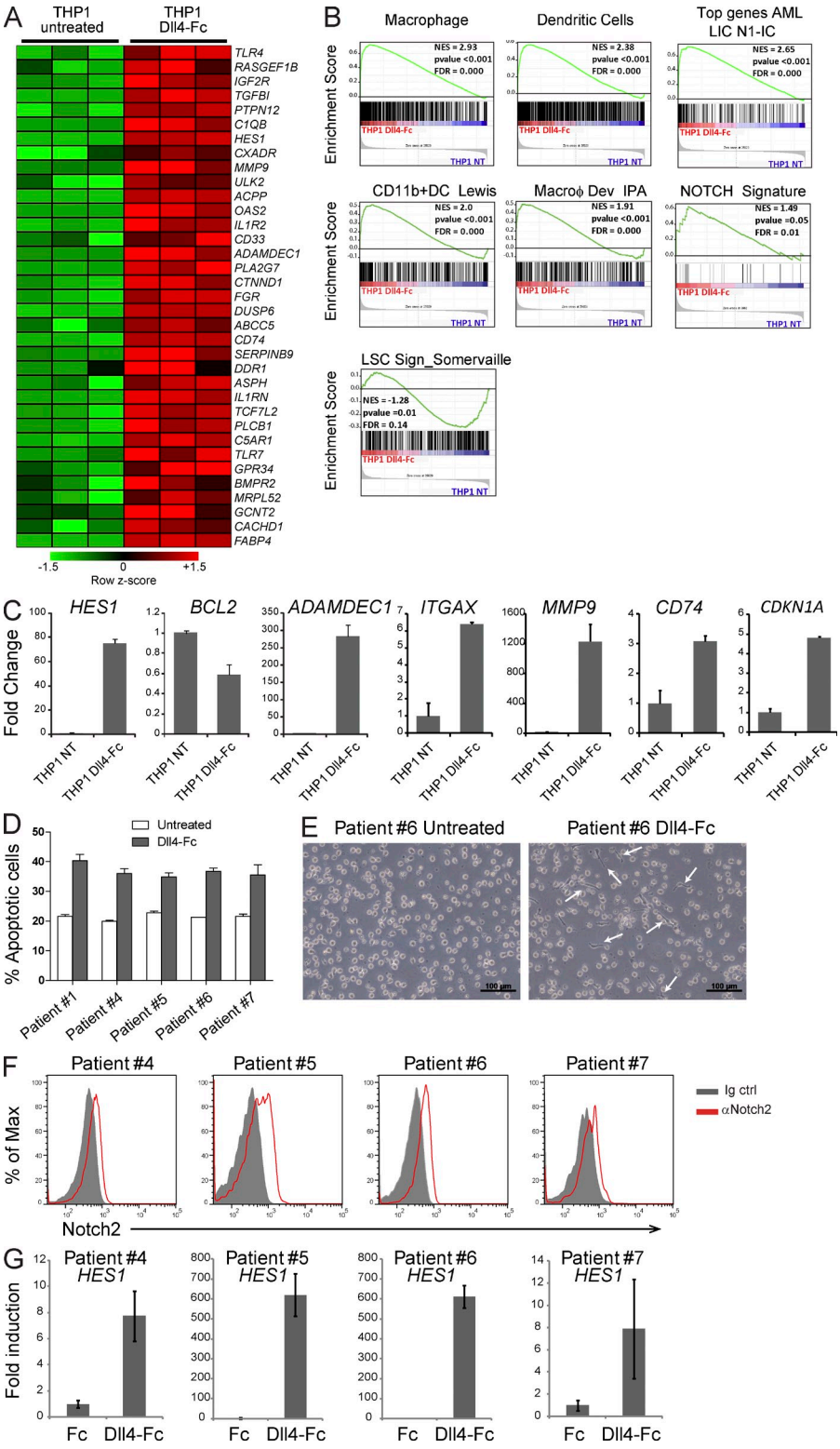

Figure 8. Recombinant Dll4-Fc ligand–mediated Notch activation induces differentiation-associated genes in THP1 cells and differentiation and apoptosis of primary AML cells in vitro. (A) Heat map representing the top significantly up-regulated genes in THP1 treated with Dll4-Fc compared with vehicle-treated THP1 for 48 h. (B) GSEA for the indicated gene sets of THP1 treated with Dll4-Fc versus THP1 treated with control vehicle. (C) qRT-PCR of indicated genes on vehicle- and Dll4-Fc–treated THP1. (D) Proportion of apoptotic cells revealed by Annexin V staining of AML patient samples treated with control vehicle or Dll4-Fc for 24 h. Data represent mean ± SD of three replicates. (E) Representative brightfield pictures of AML patient #6 cells treated with vehicle or Dll4-Fc for 24 h. Arrows indicate differentiating cells. Bars, 100 µm. (F) FACS analysis using antibodies specific for extracellular domain of Notch2. (G) qRT-PCR of *HES1* gene in AML patient cells cultured on Dll4-Fc or control Fc for 24 h. (C and G) Data represent mean ± SD of three biological replicates.

progenitor compartment showed enlargement of the GMP compartment in both relative proportion and absolute number (Fig. 9, G and H). *Ncstn*$^{-/-}$*Tet2*$^{-/-}$ compound animals eventually died after a mean of 26 wk after birth, whereas most of the WT, *Ncstn*$^{-/-}$, and *Tet2*$^{-/-}$ littermates survived (Fig. 9 I).

To address whether the induced disease is transplantable, total spleen tumor cells from *Ncstn*$^{-/-}$*Tet2*$^{-/-}$ or *Ncstn*$^{-/-}$ littermate mice (used as control) were transplanted in lethally irradiated congenic recipient mice together with a radioprotective dose of WT BM. Despite myeloid bias that was cell autonomous

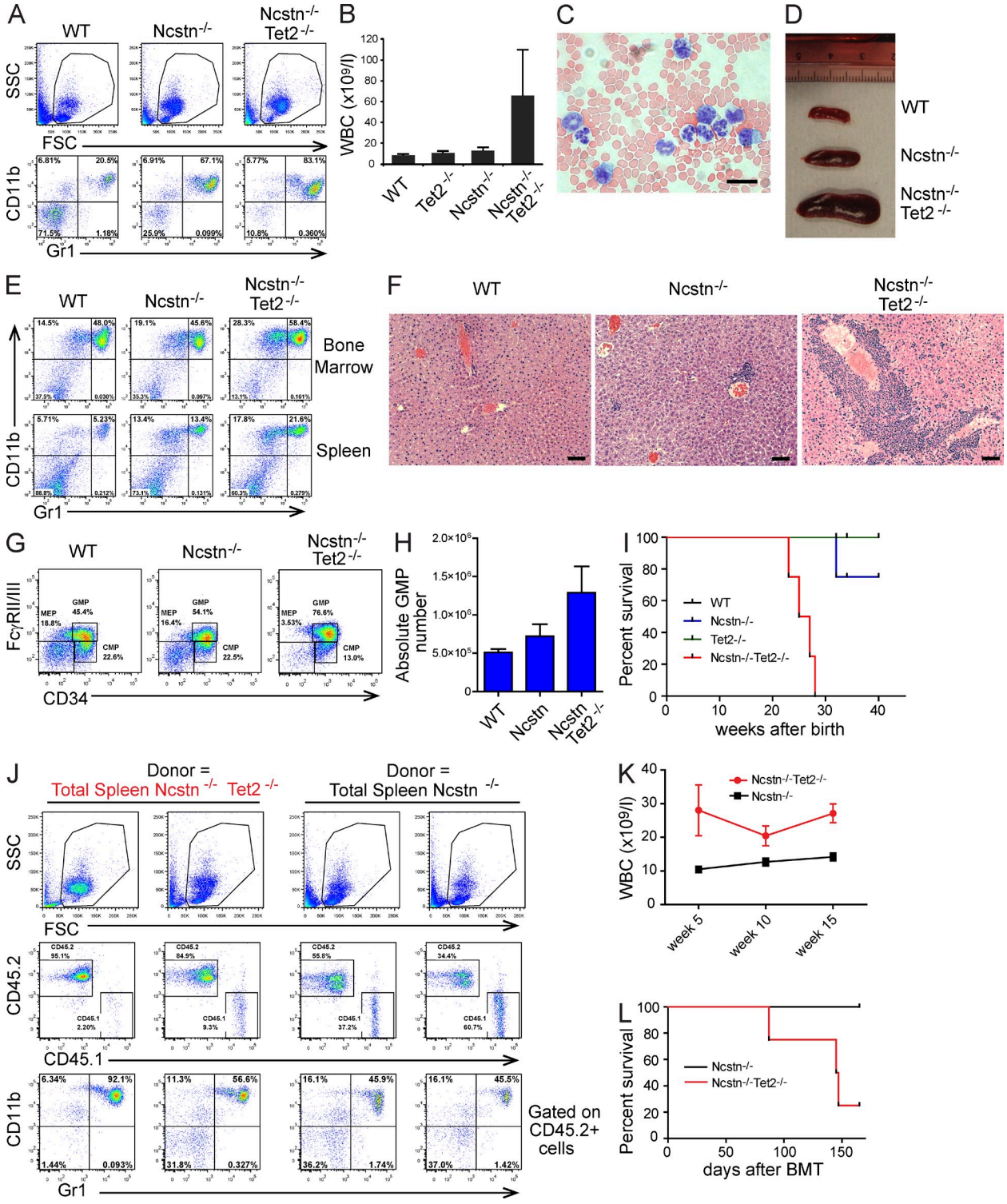

Figure 9. Notch loss of function cooperates with Tet2 loss of function to induce AML in vivo. (A) Representative FACS analysis of myeloid cells from peripheral blood of WT, Ncstn$^{-/-}$, and Ncstn$^{-/-}$Tet2$^{-/-}$ littermates 7 wk after birth. (B) Peripheral white blood cell counts of WT, Tet2$^{-/-}$, Ncstn$^{-/-}$, and Ncstn$^{-/-}$Tet2$^{-/-}$ mice 7 wk after birth. Data represent mean ± SD of five different mice per cohort. (C) Representative Wright-Giemsa–stained blood smear of Ncstn$^{-/-}$Tet2$^{-/-}$ mouse 7 wk after birth. (D) Representative spleen picture of WT, Ncstn$^{-/-}$, and Ncstn$^{-/-}$Tet2$^{-/-}$ littermates 7 wk after birth. (E) Representative FACS analysis of myeloid cells from BM and spleen of WT, Ncstn$^{-/-}$, and Ncstn$^{-/-}$Tet2$^{-/-}$ littermates 7 wk after birth. (F) H&E staining of liver sections of WT, Ncstn$^{-/-}$, and Ncstn$^{-/-}$Tet2$^{-/-}$ littermates 7 wk after birth. Bars: (C) 50 µm; (F) 200 µm. (G) Representative FACS analysis of BM myeloid progenitors (Lineage^{-}/Sca1^{-}/cKit^{+}) showing CMPs (common myeloid progenitors; CD34^{+}, FcγRII/III^{lo}), MEPs (megakaryocyte/erythrocyte progenitors; CD34^{-}/FcγRII/III^{-}), and GMPs (CD34^{+}/FcγRII/III^{+}) of WT, Ncstn$^{-/-}$, and Ncstn$^{-/-}$Tet2$^{-/-}$ littermates 7 wk after birth. (H) BM GMP absolute cell

(Fig. 9 J), *Ncstn*$^{-/-}$ cells failed to induce lethal disease in transplanted mice. *Ncstn*$^{-/-}$*Tet2*$^{-/-}$ splenocytes outcompeted WT support BM and led to elevated blood counts, starting as early as 5 wk after transplantation (Fig. 9 K). Approximately 75% of animals transplanted with *Ncstn*$^{-/-}$*Tet2*$^{-/-}$ splenocytes died within 150 d after transplantation, whereas animals transplanted with *Ncstn*$^{-/-}$ splenocytes showed increased myeloid cell counts in peripheral blood but did not develop lethal myeloid leukemia (Fig. 9 L). These results show that silencing of Notch signaling can cooperate with additional genetic lesions and lead to the rapid induction of transplantable myeloid disease reminiscent of human AML and therefore demonstrate that Notch signaling can function as a tumor suppressor.

DISCUSSION

Our study demonstrates that the Notch signaling pathway is silenced in both human and mouse AML and that this suppression is evident also in AML LICs in an MLL-AF9–induced mouse model of AML as well as in the stem and progenitor cell compartment of AML patients that likely contains LICs. We show that Notch pathway silencing in AML is in part caused by increased levels of H3K27me3 on Notch target promoters, a histone mark associated with transcriptional repression. These experiments suggested that Notch pathway inactivation is mediated by reversible epigenetic silencing. Indeed, we were able to show that Notch pathway reactivation, either through inducible expression of Notch-IC transgenes or by treatment with Dll4-Fc fusion molecules, efficiently targets both human and mouse AML, leading to growth inhibition, differentiation, and cell death. Pathway reactivation could thus be an effective therapeutic approach in AML. In agreement with this notion, we demonstrated that AML cells and most importantly AML-initiating cells uniformly express the NOTCH2 receptor, which allows for Notch pathway reactivation. Most importantly, we demonstrate that Notch2-mediated pathway reactivation fails to induce T cell leukemia. This last finding conflicts with an earlier study in which virally driven NOTCH2-IC led to T-ALL (Witt et al., 2003). However, that was an artificial system that led to nonphysiological expression levels, unlike our monoallelic, Rosa26-driven model used here, which closer mimics the physiological situation. We therefore believe that reversible Notch pathway activation, through NOTCH2 receptor (i.e., using NOTCH2-specific agonistic antibodies), could indeed be a specific, viable therapeutic approach and could also target AML-initiating cells. Similar approaches using NOTCH1-activating antibodies have been previously successfully tested in an animal study of tissue regeneration (Conboy et al., 2003).

However, it is unlikely that NOTCH2 expression is a "genetic switch" placed on stem and progenitor cells to merely suppress their ability to generate leukemia. Based on our previous study of Notch function in the BM (Klinakis et al., 2011), we believe that defined Notch expression levels and pathway activation can control cellular differentiation during early hematopoiesis. In agreement with this notion, we observed that Notch pathway reactivation led to ectopic differentiation of both mouse and human AML cells toward the macrophage and dendritic lineages. In agreement with these findings, Lewis et al. (2011) have recently suggested key roles for the Notch pathway in the differentiation of DCs from BM progenitors. Further mapping of Notch receptor expression and activation in the BM is essential for the complete understanding of Notch-regulated programs of differentiation during early hematopoiesis.

We have previously shown that Notch signaling inactivation can lead to myeloproliferative disease in mouse models but not overt AML (Klinakis et al., 2011). In an identical fashion, Tet2 mutations lead to similar CMML-like disease that only infrequently develops to AML (Moran-Crusio et al., 2011; Quivoron et al., 2011). Strikingly, combinatorial silencing of both genes leads to rapid and transplantable disease reminiscent of human AML. At this point, the mechanisms of cooperation between Notch and Tet2 silencing remain elusive. However, two recent studies using DNA methylation and gene expression analyses in human patient samples and a mouse model of myeloid leukemia induced by the IDH1R132H mutant show that several Notch target genes and Notch pathway genes are hypermethylated and silenced in IDH1/2 mutant AML (Akalin et al., 2012; Sasaki et al., 2012). As it has been shown that IDH1/2 acts upstream of Tet2 and that IDH1/2 and Tet2 mutations are mutually exclusive in AML (Figueroa et al., 2010), one can hypothesize that IDH1/2 or Tet2 mutations will impinge on a set of Notch targets and help to either maintain their silencing or silence them further. As several Notch target genes are also under the control of multiple transcription factors, hypermethylation of these genes caused by IDH/Tet2 mutations could block their reactivation. This is the first demonstration of genetic cooperation between the two pathways and the first genetic event cooperating with Tet2 loss in vivo. It also suggests that targeting both the Notch pathway and disrupting the aberrant DNA methylation, characteristic of TET2 deficiency (i.e., using hypomethylating agents) could represent a powerful combinatorial therapeutic approach in AML.

In summary, we provide here the first example of antitumor activity of Notch pathway reactivation and suggest that

number of WT, Ncstn$^{-/-}$, and Ncstn$^{-/-}$Tet2$^{-/-}$ mice 7 wk after birth. Data represent mean ± SD of three different mice per cohort. (I) Kaplan-Meier survival analysis of mice of the indicated genotypes (n = 4 per cohort). (J) Representative FACS analysis of chimerism and myeloid cells from peripheral blood of mice transplanted with 2 × 10^6 splenocytes from Ncstn$^{-/-}$ and Ncstn$^{-/-}$Tet2$^{-/-}$ (CD45.2) and 5 × 10^5 WT support BM cells (CD45.1), 10 wk after transplantation. Two mice per cohort are shown. (K) Evolution of peripheral white blood cell count in the two cohorts of transplanted mice. Data are representative of mean ± SD (Ncstn$^{-/-}$ cohort n = 6; Ncstn$^{-/-}$Tet2$^{-/-}$ cohort n = 4). (L) Kaplan-Meier survival analysis of the two cohorts of transplanted mice.

therapeutic approaches using Notch-activating ligand, agonistic Notch receptor–specific antibodies, or small molecule agonists may have potent activity in the treatment of certain subtypes of AML, particularly acute myelomonocytic leukemias by targeting AML-initiating cells. The specific surface expression of NOTCH2 could potentially maximize specificity of targeting and minimize potential side effects. Moreover, as Notch has been recently suggested to play a tumor suppressor role in several solid tumors (Agrawal et al., 2011; Lobry et al., 2011; Stransky et al., 2011; Viatour et al., 2011), Notch receptor–specific activation could therefore constitute a novel effective therapy in a wide spectrum of human malignancies.

MATERIALS AND METHODS

Animals. All animals were kept in the New York University (NYU) specific pathogen–free facility. Genotyping of $Ncstn^{f/f}$, $Tet2^{f/f}$, and $EF1a^{wt/lslN1\text{-}IC}$ was performed as previously described (Klinakis et al., 2011; Moran-Crusio et al., 2011). ROSA26-ICN(1–4) mice were generated by insertion of a loxP flanked splice acceptor NEO-ATG cassette with two polyA sites followed by ICN2 into the ROSA26 locus, allowing the ROSA26 promoter to drive expression of the NEO-ATG cassette. Cre recombinase–mediated excision of NEO-ATG results in use of the splice acceptor in the ICN2 cassette and irreversible expression of the transgene. $Ncstn^{f/f}$ and $Tet2^{f/f}$ mice were crossed to the Vav1-cre deleter strain (Stadtfeld and Graf, 2005). $EF1a^{wt/lslN1\text{-}IC}$ mice were crossed to the tamoxifen-inducible ROSA26-CreERT2 (gift from D. Littman, NYU School of Medicine, New York, NY). Tamoxifen (Sigma-Aldrich) was solubilized in corn oil (Sigma-Aldrich) at a concentration of 20 mg/ml and injected intraperitoneally at 0.2 mg/g body weight. All animal experiments were performed in accordance with the guidelines of the NYU School of Medicine Institutional Animal Care and Use Committee.

Antibodies and FACS analysis. Antibody staining and FACS analysis were performed as previously described (Klinakis et al., 2011). To analyze and isolate AML LICs and GMPs, total BM cells were recovered from flushing the tibias and femurs of mice with PBS supplemented with 3% FBS and 1% penicillin/streptomycin. BM mononuclear cells were then stained with a lineage cocktail comprised of antibodies targeting CD4, CD8, B220, NK1.1, Gr-1, CD11b, Ter119, and IL-7Rα. Cells were also stained with antibodies against cKit, Sca-1, FcγRII/III, and CD34. Cell populations were analyzed using a FACS Fortessa (BD) and sorted with a FACSAria instrument (BD). All antibodies were purchased from BD or eBioscience. We used the following antibodies: c-kit (2B8), Sca-1 (D7), Mac-1/CD11b (M1/70), Gr-1 (RB6-8C5), NK1.1 (PK136), Ter-119, IL7Rα (A7R34), CD34 (RAM34), FcγRII/III (2.4G2), CD4 (RM4-5), CD4 (H129.19), CD8 (53–6.7), CD45.1 (A20), CD45.2 (104), CD11c (HL3), NOTCH1 (APC conjugated, 22E5; eBioscience), and NOTCH2 (PE conjugated, 16F11; eBioscience). For ChIP, antibodies were purchased from Millipore (H3K27me3) and Active Motif (H3K4me3, Ezh2). Magnetic protein G beads were purchased from Invitrogen.

RT-PCR. Total RNA was isolated using the RNeasy Plus Mini kit (QIAGEN), and cDNA was synthesized using the SuperScript First-Strand kit (Invitrogen). qPCR was performed using SYBR green iMaster and a LightCycler 480 (Roche) using the primers referenced in Table S1.

Cell cross-linking and preparation of mononucleosome-containing chromatin. The cells were fixed with 1% formaldehyde for 10 min at room temperature and incubated in buffer A (10 mM Hepes, pH 7.5, 10 mM KCl, 1.5 mM $MgCl_2$, and 0.2 mM glycerol), followed by addition of NP-40 in a final concentration of 0.5% and stirring. The nuclei were isolated by centrifugation and washed once with "digest" buffer (10 mM NaCl, 10 mM Tris-HCl, pH 7.5, 3 mM $MgCl_2$, 1 mM $CaCl_2$, and 0.1 mM PMSF), followed by incubation with Micrococcal nuclease (from USB) in digest buffer at 37°C to generate mononucleosomal particles. The reaction was stopped with the addition of 20 mM EDTA, and the nuclei were lysed using the "Nuclei lysis" buffer (50 mM Tis-HCL, pH 80, 10 mM EDTA, pH 8.0, and 1% SDS) followed by sonication (2.5 min in total) using the bioruptor from Diagenode and addition of 9 vol of "IP dilution" buffer (0.01% SDS, 1.1% Triton X-100, 1.2 mM EDTA, pH 8.0, 16.7 mM Tris-HCl, pH 8.0, and 167 mM NaCl) and addition of the magnetic Dynal beads (preclearing of chromatin).

ChIP. We used standard ChIP-Seq procedures (Barski et al., 2007; Wang et al., 2008) adapted to our cell numbers (~1–5 × 10^6 cells). The antibody was incubated with the beads for 4 h in IP dilution buffer. The complex was added to the chromatin followed by overnight incubation. The complexes bound on the beads were washed with buffers (wash A: 20 mM Tris-HCl, pH 8, 150 mM NaCl, 2 mM EDTA, 1% wt/vol Triton, and 0.1% wt/vol SDS; wash B: 20 mM Tris-HCl, pH 8, 500 mM NaCl, 2 mM EDTA, 1% wt/vol Triton, and 0.1% wt/vol SDS) having increasing concentration of NaCl, once with wash buffer C (10 mM Tris-HCl, pH 8, 250 mM LiCl, 1 mM EDTA, 1% wt/vol Nonidet P-40, and 1% wt/vol deoxycholic acid), and twice with TE buffer (10 mM Tris, pH 8, and 1 mM EDTA). The precipitated DNA was cleaned with treatment with proteinase K at 65°C overnight and phenol/chloroform extraction.

ChIP-Seq. ChIP-Seq analysis of LSK and AML LICs was previously described (Bernt et al., 2011), and data are available from the GEO database under accession no. GSE29130.

BM transplantation assays. 2 × 10^6 total spleen cells from $Ncstn^{-/-}$ or $Ncstn^{-/-}Tet2^{-/-}$ mice ($Ly5.2^+$) and 5 × 10^5 total BM cells from congenic BL6SJL mice ($Ly5.1^+$) were transplanted by retroorbital i.v. injections into lethally irradiated (two times 550 cGy separated by 4 h) BL6SJL ($Ly5.1^+$) recipient mice. Peripheral blood of recipient mice was collected at 5, 10, and 15 wk after transplant.

Retroviral infection of $Lineage^-cKit^+$ BM cells and transplantation. BM cells were enriched for cKit-positive cells using the EasySep kit (STEMCELL Technologies) and cultured in OPTI-MEM supplemented with 10% FBS, 100 μ/ml penicillin, 100 μg/ml streptomycin, 50 ng/ml of SCF, 10 ng/ml IL6, and 10 ng/ml IL3. For retroviral production, Plat-E cells were transfected with MIG-MLL-AF9 by calcium phosphate method. Virus supernatant was collected 48 h after transfection and used directly for spin infection of cKit-positive enriched BM cells at 2,500 rpm for 90 min. 48 h after infection, lineage-negative GFP-positive cells were sorted for transplantation. 50,000 sorted cell were mixed with 5 × 10^5 total BM cells from congenic BL6SJL mice ($Ly5.1^+$) and transplanted by retroorbital i.v. injections into lethally irradiated (two times 550 cGy separated by 4 h) BL6SJL ($Ly5.1^+$) recipient mice.

Comparison of N1-IC and N2-IC expression in hematopoietic system. ROSA26-ICN mice were crossed to UbcCreER mice, and BM cells were isolated by flushing bones with a solution of PBS complemented with 3% FBS. 2 × 10^6 total BM cells were resuspended in 100 ml PBS and kept on ice until retroorbital injection into lethally irradiated (two times 550 Gy) WT CD45.2 recipients. 4 wk after reconstitution, ICN expression was induced via three consecutive intraperitoneal injections of tamoxifen daily at a dose of 0.2 mg/g mouse. 2, 4, and 6 wk after the last injection, peripheral blood was analyzed and animals were followed for survival.

In vitro differentiation assays. 500 sorted AML LICs were plated in triplicates into cytokine-supplemented methylcellulose medium (MethoCult 3434; STEMCELL Technologies) in the presence of 250 nM 4OHT or vehicle DMSO. Colony number was scored after 8 d of culture. Cells were recovered 8 d later, stained, and analyzed by FACS as described in Antibodies and FACS analysis.

Cell cultures and Dll4-Fc stimulation. Mouse AML LICs were cultured in OPTI-MEM supplemented with 10% FBS, 100 μ/ml penicillin, 100 μg/ml streptomycin, 50 ng/ml SCF, 10 ng/ml IL6, and 10 ng/ml IL3 for 24 or 48 h.

Human cell lines THP1, U937, Loucy, and KOPTK were cultured in RPMI with 10% FBS, 100 µ/ml penicillin, and 100 µg/ml streptomycin. Human primary AML samples were cultured in serum-free expansion medium (STEMCELL Technologies) supplemented with 100 ng/ml SCF, 50 ng/ml TPO, 50 ng/ml FLT3L, 20 ng/ml IL6, and 20 ng/ml IL3 for 24 h. Mouse and human cytokines were purchased from PeproTech. For Dll4-Fc and Fc stimulation, tissue culture plates were coated overnight with a solution of PBS and 60 nM Dll4-Fc or Fc at 4°C and then washed with PBS before use for culture.

Cell death assays. Cells were stained with Annexin V and 7AAD according to the manufacturer's instructions (BD) to assess levels of apoptosis. TUNEL assay (Millipore) was performed on 4-µm sections of paraffin-embedded tissues, deparaffinized with xylene, and stained according to the manufacturer's instructions.

Cell cycle analysis. For Ki67/DAPI staining, the cells were first treated with Fix and Perm reagents according to the manufacturer's instruction (Invitrogen), incubated with 20 µl Ki67 PE-conjugated antibody (BD) in 100 µl of solution B for 20 min, and then washed and resuspended in PBS with 5 µg/ml RNaseA and 2 µg/ml DAPI. Stained cells were analyzed using a FACS Fortessa.

Histological analyses. Mice were killed and autopsied, and then dissected tissue samples or tumors were fixed for 24 h in 10% buffered formalin, dehydrated, and embedded in paraffin. Paraffin blocks were sectioned at 4 µm and stained with hematoxylin and eosin (H&E). Images were acquired using an Axio Observer A1 microscope (Carl Zeiss).

Wright-Giemsa staining. To examine morphological changes associated with myeloid differentiation, cells were cytospun for 5 min at 500 rpm onto microscope slides. Cells were fixed and permeabilized in 100% methanol for 30 s, stained for 3 min in Wright-Giemsa stain (Thermo Fisher Scientific), stained for 10 min in 15% Wright-Giemsa stain, 1% Azure Blend (Thermo Fisher Scientific), and 84% ddH_2O, then stained for 2 min in 12% Wright-Giemsa stain and 88% phosphate buffer, pH 6.8, and then washed with ddH_20. Images were acquired using an Axio Observer A1 microscope.

Peripheral blood analysis. Blood was collected by retroorbital bleeding using heparinized micro-hematocrit capillary tubes (Thermo Fisher Scientific). Automated peripheral blood counts were obtained using a HemaVet 950 (Drew Scientific) according to standard manufacturer's instruction. Differential blood counts were realized on blood smears stained using Wright-Giemsa staining and visualized using an Axio Observer A1 microscope.

Microarray analysis. LSK, mT-ALL, and AML LICs from individual mice were used. Freshly isolated cells were sorted by surface marker expression, and total RNA was extracted using the RNeasy kit (QIAGEN). To generate sufficient sample quantities for oligonucleotide gene chip hybridization experiments, we used the Ovation RNA Amplification System V2 (Nugen) for cRNA amplification and labeling. The amplified cRNA was labeled and hybridized to the Mouse 430.2 microarrays (Affymetrix). For human THP1 cell microarrays, cRNA was labeled and hybridized to the Human HG133plus2 microarrays (Affymetrix). The Affymetrix gene expression profiling data were normalized using the previously published robust multi-array average (RMA) algorithm (Irizarry et al., 2003) using the GeneSpring GX software (Agilent Technologies). The gene expression intensity presentation was generated with MultiExperiment Viewer software (version 4.7.4). All newly generated microarray data have been deposited in the GEO database under accession no. GSE42261.

Human samples microarray analysis. AML and HSPC samples used in this study have been described previously (Metzeler et al., 2008; Verhaak et al., 2009; Gentles et al., 2010) and are available at the GEO database under accession nos. GSE6891, GSE24006, and GSE12417. Analysis was performed using R 2.14.0 and BioConductor. Raw data were generated using the RMA package. For comparison of different array sets, raw expression data were normalized to the mean of control GAPDH probe sets.

AML blast staining, purification, and expression analysis of AML samples. Mononuclear cells from AML patients were prepared using Ficoll-Paque Plus (GE Healthcare). Mononuclear fractions were stained with the following fluorochrome-conjugated antibodies (all human and all from BD): CD45RA (MEM56), CD38 (HIT2), CD90 (5E10), CD34 (581), CD123 (7G3), CD3 (S4.1), and CD19 (SJ25-C1). Cells were stained on ice, and dead cells were excluded by propidium iodide staining. Cells were sorted to >90% purity by FACS analysis.

Total RNA was extracted from FACS-sorted AML patient blast populations using the Ambion RNA Isolation kit (Applied Biosystems) and treated with DNaseI (QIAGEN). RNA samples were subjected to reverse transcription, linear amplification, production, and fragmentation of biotinylated cRNA (Affymetrix). 15 µg cRNA from each sample was hybridized to Affymetrix HG U133 Plus 2.0 microarrays.

GSEA. GSEA was performed using GSEA software (Subramanian et al., 2005; http://www.broadinstitute.org/gsea/) using Gene set as permutation type, 1,000 permutations, and log2 ratio of classes as metric for ranking genes. The DC and Macrophage differentiation gene sets were generated using a systematic approach based on the comparison of gene expression arrays from WT GMP and splenic macrophages and DCs. Genes that were significantly up-regulated in GMP compared with macrophages or DCs (over twofold induction, $P < 0.05$) were used to define differentiation signature genes. Other gene sets used in the analysis were taken from gene sets already present in the MSig Database of the Broad Institute or previously published (Somervaille et al., 2009; Lewis et al., 2011; Zuber et al., 2011).

Statistical analysis. The means of each dataset were analyzed using the Student's *t* test, with a two-tailed distribution and assuming equal sample variance. Statistical analysis of Kaplan-Meier survival curve was performed using the Gehan-Breslow-Wilcoxon test.

Online supplemental material. Table S1 lists sequence of primers used for qRT-PCR and ChIP. Table S2 lists characteristics of patients used for AML stem cell expression arrays. Online supplemental material is available at http://www.jem.org/cgi/content/full/jem.20121484/DC1.

We would like to thank members of the Aifantis Laboratory for discussions and comments, Dr. J. Zavadil and the New York University (NYU) Genome Technology Center (supported in part by National Institutes of Health [NIH]/National Cancer Institute [NCI grant P30 CA016087-30) for expert assistance with microarray experiments, the NYU Flow Cytometry facility (supported in part by NIH/NCI grant 5 P30CA16087-31) for expert cell sorting, the NYU Histology Core (grant 5P30CA16087-31), and the Transgenic Mouse Core (NYU Cancer Institute Center grant 5P30CA16087-31).

I. Aifantis was supported by the NIH (grants RO1CA133379, RO1CA105129, R21CA141399, RO1CA149655, and RO1GM088847), the Leukemia & Lymphoma Society, the V Foundation for Cancer Research, the St. Baldrick's Foundation for Cancer Research, and the Irma T. Hirschl Trust. C. Lobry is supported by the NYU Kimmel Stem Cell Institute and is a Leukemia & Lymphoma Society Special Fellow. P. Ntziachristos is supported by a Lady Tata Foundation Award. I. Aifantis is a Howard Hughes Medical Institute Early Career Scientist.

The authors declare no competing financial interests.

Submitted: 9 July 2012
Accepted: 5 December 2012

REFERENCES

Abdel-Wahab, O., A. Mullally, C. Hedvat, G. Garcia-Manero, J. Patel, M. Wadleigh, S. Malinge, J. Yao, O. Kilpivaara, R. Bhat, et al. 2009. Genetic characterization of TET1, TET2, and TET3 alterations in myeloid malignancies. *Blood*. 114:144–147. http://dx.doi.org/10.1182/blood-2009-03-210039

Agrawal, N., M.J. Frederick, C.R. Pickering, C. Bettegowda, K. Chang, R.J. Li, C. Fakhry, T.X. Xie, J. Zhang, J. Wang, et al. 2011. Exome sequencing of head and neck squamous cell carcinoma reveals inactivating mutations in NOTCH1. *Science*. 333:1154–1157. http://dx.doi.org/10.1126/science.1206923

Akalin, A., F.E. Garrett-Bakelman, M. Kormaksson, J. Busuttil, L. Zhang, I. Khrebtukova, T.A. Milne, Y. Huang, D. Biswas, J.L. Hess, et al. 2012. Base-pair resolution DNA methylation sequencing reveals profoundly divergent epigenetic landscapes in acute myeloid leukemia. *PLoS Genet*. 8:e1002781. http://dx.doi.org/10.1371/journal.pgen.1002781

Armstrong, S.A., T.R. Golub, and S.J. Korsmeyer. 2003. MLL-rearranged leukemias: insights from gene expression profiling. *Semin. Hematol*. 40: 268–273. http://dx.doi.org/10.1016/S0037-1963(03)00196-3

Artavanis-Tsakonas, S., M.D. Rand, and R.J. Lake. 1999. Notch signaling: cell fate control and signal integration in development. *Science*. 284:770–776. http://dx.doi.org/10.1126/science.284.5415.770

Bacher, U., S. Schnittger, and T. Haferlach. 2010. Molecular genetics in acute myeloid leukemia. *Curr. Opin. Oncol*. 22:646–655. http://dx.doi.org/10.1097/CCO.0b013e32833ed806

Barski, A., S. Cuddapah, K. Cui, T.Y. Roh, D.E. Schones, Z. Wang, G. Wei, I. Chepelev, and K. Zhao. 2007. High-resolution profiling of histone methylations in the human genome. *Cell*. 129:823–837. http://dx.doi.org/10.1016/j.cell.2007.05.009

Bernt, K.M., N. Zhu, A.U. Sinha, S. Vempati, J. Faber, A.V. Krivtsov, Z. Feng, N. Punt, A. Daigle, L. Bullinger, et al. 2011. MLL-rearranged leukemia is dependent on aberrant H3K79 methylation by DOT1L. *Cancer Cell*. 20:66–78. http://dx.doi.org/10.1016/j.ccr.2011.06.010

Buonamici, S., T. Trimarchi, M.G. Ruocco, L. Reavie, S. Cathelin, B.G. Mar, A. Klinakis, Y. Lukyanov, J.C. Tseng, F. Sen, et al. 2009. CCR7 signalling as an essential regulator of CNS infiltration in T-cell leukaemia. *Nature*. 459:1000–1004. http://dx.doi.org/10.1038/nature08020

Conboy, I.M., M.J. Conboy, G.M. Smythe, and T.A. Rando. 2003. Notch-mediated restoration of regenerative potential to aged muscle. *Science*. 302:1575–1577. http://dx.doi.org/10.1126/science.1087573

Dahlberg, A., C. Delaney, and I.D. Bernstein. 2011. Ex vivo expansion of human hematopoietic stem and progenitor cells. *Blood*. 117:6083–6090. http://dx.doi.org/10.1182/blood-2011-01-283606

Dash, A., and D.G. Gilliland. 2001. Molecular genetics of acute myeloid leukaemia. *Best Pract. Res. Clin. Haematol*. 14:49–64. http://dx.doi.org/10.1053/beha.2000.0115

de Pooter, R.F., T.M. Schmitt, J.L. de la Pompa, Y. Fujiwara, S.H. Orkin, and J.C. Zúñiga-Pflücker. 2006. Notch signaling requires GATA-2 to inhibit myelopoiesis from embryonic stem cells and primary hemopoietic progenitors. *J. Immunol*. 176:5267–5275.

Delaney, C., S. Heimfeld, C. Brashem-Stein, H. Voorhies, R.L. Manger, and I.D. Bernstein. 2010. Notch-mediated expansion of human cord blood progenitor cells capable of rapid myeloid reconstitution. *Nat. Med*. 16:232–236. http://dx.doi.org/10.1038/nm.2080

Delhommeau, F., S. Dupont, V. Della Valle, C. James, S. Trannoy, A. Massé, O. Kosmider, J.P. Le Couedic, F. Robert, A. Alberdi, et al. 2009. Mutation in TET2 in myeloid cancers. *N. Engl. J. Med*. 360:2289–2301. http://dx.doi.org/10.1056/NEJMoa0810069

Döhner, H., E.H. Estey, S. Amadori, F.R. Appelbaum, T. Büchner, A.K. Burnett, H. Dombret, P. Fenaux, D. Grimwade, R.A. Larson, et al; European LeukemiaNet. 2010. Diagnosis and management of acute myeloid leukemia in adults: recommendations from an international expert panel, on behalf of the European LeukemiaNet. *Blood*. 115:453–474. http://dx.doi.org/10.1182/blood-2009-07-235358

Figueroa, M.E., O. Abdel-Wahab, C. Lu, P.S. Ward, J. Patel, A. Shih, Y. Li, N. Bhagwat, A. Vasanthakumar, H.F. Fernandez, et al. 2010. Leukemic IDH1 and IDH2 mutations result in a hypermethylation phenotype, disrupt TET2 function, and impair hematopoietic differentiation. *Cancer Cell*. 18:553–567. http://dx.doi.org/10.1016/j.ccr.2010.11.015

Fröhling, S., C. Scholl, D.G. Gilliland, and R.L. Levine. 2005. Genetics of myeloid malignancies: pathogenetic and clinical implications. *J. Clin. Oncol*. 23:6285–6295. http://dx.doi.org/10.1200/JCO.2005.05.010

Gentles, A.J., S.K. Plevritis, R. Majeti, and A.A. Alizadeh. 2010. Association of a leukemic stem cell gene expression signature with clinical outcomes in acute myeloid leukemia. *JAMA*. 304:2706–2715. http://dx.doi.org/10.1001/jama.2010.1862

Ilagan, M.X., and R. Kopan. 2007. SnapShot: notch signaling pathway. *Cell*. 128:1246.e1–1246.e2. http://dx.doi.org/10.1016/j.cell.2007.03.011

Irizarry, R.A., B. Hobbs, F. Collin, Y.D. Beazer-Barclay, K.J. Antonellis, U. Scherf, and T.P. Speed. 2003. Exploration, normalization, and summaries of high density oligonucleotide array probe level data. *Biostatistics*. 4:249–264. http://dx.doi.org/10.1093/biostatistics/4.2.249

Klinakis, A., C. Lobry, O. Abdel-Wahab, P. Oh, H. Haeno, S. Buonamici, I. van De Walle, S. Cathelin, T. Trimarchi, E. Araldi, et al. 2011. A novel tumour-suppressor function for the Notch pathway in myeloid leukaemia. *Nature*. 473:230–233. http://dx.doi.org/10.1038/nature09999

Ko, M., H.S. Bandukwala, J. An, E.D. Lamperti, E.C. Thompson, R. Hastie, A. Tsangaratou, K. Rajewsky, S.B. Koralov, and A. Rao. 2011. Ten-Eleven-Translocation 2 (TET2) negatively regulates homeostasis and differentiation of hematopoietic stem cells in mice. *Proc. Natl. Acad. Sci. USA*. 108:14566–14571. http://dx.doi.org/10.1073/pnas.1112317108

Krivtsov, A.V., D. Twomey, Z. Feng, M.C. Stubbs, Y. Wang, J. Faber, J.E. Levine, J. Wang, W.C. Hahn, D.G. Gilliland, et al. 2006. Transformation from committed progenitor to leukaemia stem cell initiated by MLL-AF9. *Nature*. 442:818–822. http://dx.doi.org/10.1038/nature04980

Langemeijer, S.M., M.G. Aslanyan, and J.H. Jansen. 2009. TET proteins in malignant hematopoiesis. *Cell Cycle*. 8:4044–4048. http://dx.doi.org/10.4161/cc.8.24.10239

Lewis, K.L., M.L. Caton, M. Bogunovic, M. Greter, L.T. Grajkowska, D. Ng, A. Klinakis, I.F. Charo, S. Jung, J.L. Gommerman, et al. 2011. Notch2 receptor signaling controls functional differentiation of dendritic cells in the spleen and intestine. *Immunity*. 35:780–791. http://dx.doi.org/10.1016/j.immuni.2011.08.013

Li, Z., X. Cai, C.L. Cai, J. Wang, W. Zhang, B.E. Petersen, F.C. Yang, and M. Xu. 2011. Deletion of Tet2 in mice leads to dysregulated hematopoietic stem cells and subsequent development of myeloid malignancies. *Blood*. 118:4509–4518. http://dx.doi.org/10.1182/blood-2010-12-325241

Lobry, C., P. Oh, and I. Aifantis. 2011. Oncogenic and tumor suppressor functions of Notch in cancer: it's NOTCH what you think. *J. Exp. Med*. 208:1931–1935. http://dx.doi.org/10.1084/jem.20111855

Maillard, I., U. Koch, A. Dumortier, O. Shestova, L. Xu, H. Sai, S.E. Pross, J.C. Aster, A. Bhandoola, F. Radtke, and W.S. Pear. 2008. Canonical notch signaling is dispensable for the maintenance of adult hematopoietic stem cells. *Cell Stem Cell*. 2:356–366. http://dx.doi.org/10.1016/j.stem.2008.02.011

Malyukova, A., T. Dohda, N. von der Lehr, S. Akhoondi, M. Corcoran, M. Heyman, C. Spruck, D. Grandér, U. Lendahl, and O. Sangfelt. 2007. The tumor suppressor gene hCDC4 is frequently mutated in human T-cell acute lymphoblastic leukemia with functional consequences for Notch signaling. *Cancer Res*. 67:5611–5616. (published erratum appears in *Caner Res*. 2008. 68:2051) http://dx.doi.org/10.1158/0008-5472.CAN-06-4381

Maser, R.S., B. Choudhury, P.J. Campbell, B. Feng, K.-K. Wong, A. Protopopov, J. O'Neil, A. Gutierrez, E. Ivanova, I. Perna, et al. 2007. Chromosomally unstable mouse tumours have genomic alterations similar to diverse human cancers. *Nature*. 447:966–971. http://dx.doi.org/10.1038/nature05886

Mercher, T., M.G. Cornejo, C. Sears, T. Kindler, S.A. Moore, I. Maillard, W.S. Pear, J.C. Aster, and D.G. Gilliland. 2008. Notch signaling specifies megakaryocyte development from hematopoietic stem cells. *Cell Stem Cell*. 3:314–326. http://dx.doi.org/10.1016/j.stem.2008.07.010

Metzeler, K.H., M. Hummel, C.D. Bloomfield, K. Spiekermann, J. Braess, M.C. Sauerland, A. Heinecke, M. Radmacher, G. Marcucci, S.P. Whitman, et al; Cancer and Leukemia Group B; German AML Cooperative Group. 2008. An 86-probe-set gene-expression signature predicts survival in cytogenetically normal acute myeloid leukemia. *Blood*. 112:4193–4201. http://dx.doi.org/10.1182/blood-2008-02-134411

Moran-Crusio, K., L. Reavie, A. Shih, O. Abdel-Wahab, D. Ndiaye-Lobry, C. Lobry, M.E. Figueroa, A. Vasanthakumar, J. Patel, X. Zhao, et al. 2011. Tet2 loss leads to increased hematopoietic stem cell self-renewal and myeloid transformation. *Cancer Cell*. 20:11–24. http://dx.doi.org/10.1016/j.ccr.2011.06.001

Ntziachristos, P., A. Tsirigos, P. Van Vlierberghe, J. Nedjic, T. Trimarchi, M.S. Flaherty, D. Ferres-Marco, V. da Ros, Z. Tang, J. Siegle, et al. 2012. Genetic inactivation of the polycomb repressive complex 2 in

T cell acute lymphoblastic leukemia. *Nat. Med.* 18:298–301. http://dx.doi.org/10.1038/nm.2651

Palomero, T., W.K. Lim, D.T. Odom, M.L. Sulis, P.J. Real, A. Margolin, K.C. Barnes, J. O'Neil, D. Neuberg, A.P. Weng, et al. 2006. NOTCH1 directly regulates c-MYC and activates a feed-forward-loop transcriptional network promoting leukemic cell growth. *Proc. Natl. Acad. Sci. USA.* 103:18261–18266. http://dx.doi.org/10.1073/pnas.0606108103

Pear, W.S., J.C. Aster, M.L. Scott, R.P. Hasserjian, B. Soffer, J. Sklar, and D. Baltimore. 1996. Exclusive development of T cell neoplasms in mice transplanted with bone marrow expressing activated Notch alleles. *J. Exp. Med.* 183:2283–2291. http://dx.doi.org/10.1084/jem.183.5.2283

Quivoron, C., L. Couronné, V. Della Valle, C.K. Lopez, I. Plo, O. Wagner-Ballon, M. Do Cruzeiro, F. Delhommeau, B. Arnulf, M.H. Stern, et al. 2011. TET2 inactivation results in pleiotropic hematopoietic abnormalities in mouse and is a recurrent event during human lymphomagenesis. *Cancer Cell.* 20:25–38. http://dx.doi.org/10.1016/j.ccr.2011.06.003

Robert-Moreno, A., J. Guiu, C. Ruiz-Herguido, M.E. López, J. Inglés-Esteve, L. Riera, A. Tipping, T. Enver, E. Dzierzak, T. Gridley, et al. 2008. Impaired embryonic haematopoiesis yet normal arterial development in the absence of the Notch ligand Jagged1. *EMBO J.* 27:1886–1895. http://dx.doi.org/10.1038/emboj.2008.113

Sasaki, M., C.B. Knobbe, J.C. Munger, E.F. Lind, D. Brenner, A. Brüstle, I.S. Harris, R. Holmes, A. Wakeham, J. Haight, et al. 2012. IDH1(R132H) mutation increases murine haematopoietic progenitors and alters epigenetics. *Nature.* 488:656–659. http://dx.doi.org/10.1038/nature11323

Schroeder, T., H. Kohlhof, N. Rieber, and U. Just. 2003. Notch signaling induces multilineage myeloid differentiation and up-regulates PU.1 expression. *J. Immunol.* 170:5538–5548.

Somervaille, T.C., C.J. Matheny, G.J. Spencer, M. Iwasaki, J.L. Rinn, D.M. Witten, H.Y. Chang, S.A. Shurtleff, J.R. Downing, and M.L. Cleary. 2009. Hierarchical maintenance of MLL myeloid leukemia stem cells employs a transcriptional program shared with embryonic rather than adult stem cells. *Cell Stem Cell.* 4:129–140. http://dx.doi.org/10.1016/j.stem.2008.11.015

Stadtfeld, M., and T. Graf. 2005. Assessing the role of hematopoietic plasticity for endothelial and hepatocyte development by non-invasive lineage tracing. *Development.* 132:203–213. http://dx.doi.org/10.1242/dev.01558

Stransky, N., A.M. Egloff, A.D. Tward, A.D. Kostic, K. Cibulskis, A. Sivachenko, G.V. Kryukov, M.S. Lawrence, C. Sougnez, A. McKenna, et al. 2011. The mutational landscape of head and neck squamous cell carcinoma. *Science.* 333:1157–1160. http://dx.doi.org/10.1126/science.1208130

Subramanian, A., P. Tamayo, V.K. Mootha, S. Mukherjee, B.L. Ebert, M.A. Gillette, A. Paulovich, S.L. Pomeroy, T.R. Golub, E.S. Lander, and J.P. Mesirov. 2005. Gene set enrichment analysis: a knowledge-based approach for interpreting genome-wide expression profiles. *Proc. Natl. Acad. Sci. USA.* 102:15545–15550. http://dx.doi.org/10.1073/pnas.0506580102

Tan-Pertel, H.T., L. Walker, D. Browning, A. Miyamoto, G. Weinmaster, and J.C. Gasson. 2000. Notch signaling enhances survival and alters differentiation of 32D myeloblasts. *J. Immunol.* 165:4428–4436.

Thompson, B.J., S. Buonamici, M.L. Sulis, T. Palomero, T. Vilimas, G. Basso, A. Ferrando, and I. Aifantis. 2007. The SCF^{FBW7} ubiquitin ligase complex as a tumor suppressor in T cell leukemia. *J. Exp. Med.* 204:1825–1835. http://dx.doi.org/10.1084/jem.20070872

Verhaak, R.G., B.J. Wouters, C.A. Erpelinck, S. Abbas, H.B. Beverloo, S. Lugthart, B. Löwenberg, R. Delwel, and P.J. Valk. 2009. Prediction of molecular subtypes in acute myeloid leukemia based on gene expression profiling. *Haematologica.* 94:131–134. http://dx.doi.org/10.3324/haematol.13299

Viatour, P., U. Ehmer, L.A. Saddic, C. Dorrell, J.B. Andersen, C. Lin, A.F. Zmoos, P.K. Mazur, B.E. Schaffer, A. Ostermeier, et al. 2011. Notch signaling inhibits hepatocellular carcinoma following inactivation of the RB pathway. *J. Exp. Med.* 208:1963–1976. http://dx.doi.org/10.1084/jem.20110198

Vo, T.T., J. Ryan, R. Carrasco, D. Neuberg, D.J. Rossi, R.M. Stone, D.J. Deangelo, M.G. Frattini, and A. Letai. 2012. Relative mitochondrial priming of myeloblasts and normal HSCs determines chemotherapeutic success in AML. *Cell.* 151:344–355. http://dx.doi.org/10.1016/j.cell.2012.08.038

Wang, Z., C. Zang, J.A. Rosenfeld, D.E. Schones, A. Barski, S. Cuddapah, K. Cui, T.Y. Roh, W. Peng, M.Q. Zhang, and K. Zhao. 2008. Combinatorial patterns of histone acetylations and methylations in the human genome. *Nat. Genet.* 40:897–903. http://dx.doi.org/10.1038/ng.154

Wang, H., J. Zou, B. Zhao, E. Johannsen, T. Ashworth, H. Wong, W.S. Pear, J. Schug, S.C. Blacklow, K.L. Arnett, et al. 2011. Genome-wide analysis reveals conserved and divergent features of Notch1/RBPJ binding in human and murine T-lymphoblastic leukemia cells. *Proc. Natl. Acad. Sci. USA.* 108:14908–14913. http://dx.doi.org/10.1073/pnas.1109023108

Weng, A.P., A.A. Ferrando, W. Lee, J.P. Morris IV, L.B. Silverman, C. Sanchez-Irizarry, S.C. Blacklow, A.T. Look, and J.C. Aster. 2004. Activating mutations of NOTCH1 in human T cell acute lymphoblastic leukemia. *Science.* 306:269–271. http://dx.doi.org/10.1126/science.1102160

Witt, C.M., V. Hurez, C.S. Swindle, Y. Hamada, and C.A. Klug. 2003. Activated Notch2 potentiates CD8 lineage maturation and promotes the selective development of B1 B cells. *Mol. Cell. Biol.* 23:8637–8650. http://dx.doi.org/10.1128/MCB.23.23.8637-8650.2003

Zuber, J., J. Shi, E. Wang, A.R. Rappaport, H. Herrmann, E.A. Sison, D. Magoon, J. Qi, K. Blatt, M. Wunderlich, et al. 2011. RNAi screen identifies Brd4 as a therapeutic target in acute myeloid leukaemia. *Nature.* 478:524–528. http://dx.doi.org/10.1038/nature10334

Zúñiga-Pflücker, J.C. 2004. T-cell development made simple. *Nat. Rev. Immunol.* 4:67–72. http://dx.doi.org/10.1038/nri1257